Liquefaction Behaviour and Dynamic Soil Properties of River Channel Deposit in Kolkata City

A Thesis submitted in partial fulfilment of the requirements for the degree of

Master of Engineering

in

Civil Engineering

Submitted By

MD BAKIBILLAH

Roll No: 002210402016

Exam Roll No: M4CIV24014

Under the Guidance of

DR. NARAYAN ROY

Assistant Professor, Jadavpur University

DEPARTMENT OF CIVIL ENGINEERING

JADAVPUR UNIVERSITY

Jadavpur, Kolkata-700032

DECLARATION

I hereby declare that this thesis contains literature review and original research works by the undersigned candidate, as a part of his Master of Civil Engineering in Soil Mechanics and Foundation Engineering studies. All the information in this document has academic rules and ethical conduct.

I also declare that, as required by these rules and conduct, I have fully cited and referenced all material and results that are not original to this work.

Md. Bakibillah 31.05.2024

(Md Bakibillah)

Exam Roll No: **M4CIV24014**

Reg. No: **163466 of 2022-2023**

Class Roll No: **002210402016**

Jadavpur University

CERTIFICATE

This is to certify that Md Bakibillah bearing class roll number 002210402016 has prepared this thesistitled "**Liquefaction Behaviour and Dynamic Soil Properties of River Channel Deposit in Kolkata City**" under my supervision in the partial fulfilment of the requirements for the degree of "**Master of Engineering in Civil Engineering**" at Jadavpur University.

Date: 31/05/24

Assistant Professor
Department of Civil Engineering
Jadavpur University
Kolkata-700 032

31/05/24

(Dr. Narayan Roy)

Thesis Supervisor

Assistant Professor

Department of Civil Engineering

Jadavpur University

Countersigned by

Dipan Laha 31/5/24

DEAN

Faculty of Engineering and Technology

Jadavpur University

Kolkata-700032

DEAN
Faculty of Engineering & Technology
JADAVPUR UNIVERSITY
KOLKATA-700 032

31/5/24

H.O.D

Department of Civil Engineering

Jadavpur University

Kolkata-700032

Head
Department of Civil Engineering
Jadavpur University
Kolkata-700 032

CERTIFICATE OF APPROVAL

The foregoing thesis is hereby approved as a creditable study of an engineering subject carried out and presented in a manner satisfactory to warrant its acceptance as a prerequisite to the degree for which it has been submitted. It is understood that by this approval, the undersigned do not necessarily endorse or approve any statement made, opinion expressed and conclusion drawn therein but approve the thesis only for the purpose for which it has been submitted.

COMMITE OF FINAL EXAMINATION FOR EVALUATION OF THE THESIS WORK

1. ---------- (Signature of the Examiner)

2.----------(Signature of the Examiner)

3.----------(Signature of the Examiner)

ACKNOWLEDGEMENT

I would like to express my sincere gratitude to **Dr. Narayan Roy**, my thesis guide, Jadavpur University, for his valuable guidance, ingenious suggestions and constant encouragement throughout the course of my thesis work.I am especially thankful to **Prof. Ramendu Bikas Sahu** whose continuous support and guidance help me to complete my thesis work.I sincerely thank them for their patience and constant help whenever needed, besides their heavy workload. The consideration extended by them is deeply acknowledged.

I thank **Prof. Partha Bhattacharya**, Head of the Civil Engineering Department, for providing the necessary facilities for carrying out the project work.

I extend my heartfelt gratitude to friends for immense help during the project. I also thank lab assistants and all the fellow scholars who had taken up their valuable time to help me and endowed me with a constructive suggestion for completion of my work.

I am grateful to my parents and my brother for the tremendous understanding, encouragement and adjustment they made for me to make my work here at Jadavpur University easier.

Above all, I thank God for providing me with good health and knowledge.

Place: Jadavpur University **Md Bakibillah**

CONTENTS

List of Figures

List of Tables

Abstract

The present works studies the Liquefaction resistance and dynamic soil properties of sandy soil collected from Tollygunge region of Kolkata city. In connection with this, a series of strain controlled cyclic triaxial tests have been performed at the laboratory on prepared soil sample (75 mm diameter and 150 mm height) under undrained condition. The sample was collected from the Tollygaunge area in Kolkata city. In this work, the effect of relative density, peak shear strain and frequency of loading on dynamic behaviour of the sandy soil has been investigated.

Soil samples have been prepared using moist tamping method to achieve desired relative densities. To study the effect of relative density, the tests have been performed at four different relative densities, i.e., 35, 60, 75 and 90%. All the tests are carried out at an effective confinement of 100 kPa. For studying the effect of peak shear strain, tests have been conducted at three different peak shear strain, i.e., 0.50, 1.0 and 1.5%.The effect of frequency of loading is examined by conducting tests at 0.1, 0.5 and 1Hz frequencies with constant relative density of 60%. So, in this study a total 11 numbers of cyclic triaxial tests have been performed. The results are presented in the form of excess pore pressure ratio vs no of cycle to liquefaction, relative density of soil vs excess pore pressure ratio and cyclic shear strain vs excess pore pressure ratio. From the results, it can be observed that as the relative density of soil increases the no. of cycle for liquefaction also increases. The peak shear strain is found to have a significant effect on liquefaction resistance of soil. As the peak shear strain increases liquefaction resistance of soil drastically decreases.

In this study, the dynamic soil properties in terms of shear modulus and damping ratio have also been determined for different parametric variations. Finally, attempt has also been made to obtain the modulus reduction and damping curves for the soil and the same is proposed for the study region. These curves might play an important role to study the site specific dynamic response of the soil for the region.

1. Introduction

Liquefaction remains a critical area of research in geotechnical earthquake engineering due to its profound impact on soil stability during seismic events. The phenomenon, which involves the loss of soil strength and stiffness due to increased pore water pressure, was notably highlighted following the devastating consequences of the 1964 Alaska and Niigata earthquakes. These events underscored the necessity for understanding liquefaction in various soil types, particularly sandy soils which are most susceptible. Although significant progress has been made in this field, the complexity of liquefaction requires continuous research to fully comprehend its mechanisms, especially in varied geological contexts.

Kolkata, one of India's largest metropolitan areas, is located on the alluvial deposits of the Ganges River basin, presenting unique challenges and opportunities for geotechnical studies. The city's expansion, covering approximately 185 square kilometres and housing over 4.5 million people, has led to substantial urban development, often without proper planning. This unregulated construction on potentially liquefiable soils amplifies the importance of understanding soil behaviour under seismic loading.

The alluvial Gangetic deposit mainly forms the subsoil of Kolkata city. In the city, two different types of subsurface stratifications are observed: Normal Kolkata Deposit (NKD) and river channel deposits (RCD). In NKD, a thick layer of silty clay/clayey silt is present up to a depth of approximately 14 metres, followed by a deposit of stiff to very hard clay extending to depths of 40-50 metres with intermediate sand layers. On the other hand, along the course of the Adiganga channel, RCD is observed, characterised by medium to dense sandy deposits reaching significant depths (Roy and Sahu, 2012). Some region of the Tollygunge area, in particular, is characterised by these RCDs, which pose a notable risk for liquefaction during earthquakes.

Previous studies have explored the liquefaction behaviour of similar Gangetic sands, revealing critical insights into how variables such as silt content, confining pressure, and cyclic strain amplitude influence soil response. The effect of different percentages of silt content in sandy soils has also been extensively studied by researchers using cyclic triaxial tests (Polito and Martin, 2001; Xenaki and Athanasopoulos, 2003; Karim and Alam, 2014). Uniform clean sand deposits are rare, as these often contain varying percentages of silt. Since the behaviour of a soil deposit under cyclic loading can significantly vary depending on its composition, it is essential to characterise each type of soil under controlled laboratory conditions.

However, detailed, proper investigations for the RCD soil are limited. Recognizing the urgency for the study, this thesis aims to determine the liquefaction behaviour and dynamic soil properties of the RCD soil using high strain cyclic triaxial tests. This research will systematically investigate how relative density, cyclic shear strain amplitude and frequency of loading affect pore water pressure generation and the number of cycles required to reach liquefaction. By collecting and analysing soil samples from Tollygunge area, the study will provide valuable data on the liquefaction characteristics of the said soil.

In addition to liquefaction potential, this study also focuses on evaluating the dynamic soil properties, specifically shear modulus and damping ratio, for the RCD soil. Understanding these properties is crucial for predicting soil behaviour under cyclic loading conditions and for designing earthquake-resistant structures. The research also involves proposing a site-specific modulus reduction and damping ratio curve, which will aid in accurately modelling the soil's response to seismic activities.

1.1 Objective and scopes of the study

The objective of the work is to study the liquefaction behavior and dynamic soil properties of sandy soil of Tollygunge area in Kolkata city using strain controlled cyclic triaxial tests. The detailed scopes of the present study are as follows:

(i) The study has been performed with varying relative densities, i.e., 30%, 60%, 75% and 90%, to study the effect of relative density on liquefaction resistance and dynamic soil properties.

(ii) The effect of peak shear strain (0.5%, 1.0% and 1.5%) on liquefaction behavior and dynamic soil properties has also been studies.

(iii) The study is also conducted to obtain the effect of frequency of loading (0.1, 0.5 & 1 Hz) on liquefaction resistance of the soil collected from the study region.

1.2 Organization of the thesis

In the section 1, introduction the study has been discussed highlighting the need of the study and the origin of the study. Also the objective and the scopes are also described in this section. Section 2 consists of literature review. In this section past literatures have been reviewed and effort was made to understand the effect of various parameter i.e., relative density, confining pressure, shear strain, void ratio etc on the liquefaction behavior and the dynamic soil properties. Section 3 depicts the complete procedure of the experimental program from sample preparation to sample testing. In the section 4, results obtained from the study have been discussed and effect of various parameters such as relative density, shear strain amplitude and the loading frequency on the dynamic soil behavior have been discussed. In the section 5, conclusions have been drawn from the above discussion. Finally, References are given in the section 6.

2. Literature Review

Lade and Yamamuro (1997) conducted Undrained triaxial compression tests on reconstituted samples of Nevada and Ottawa sands with systematic variations in the fines content (particles smaller than 0.074 mm in diameter) to evaluate the effect of the finer fraction on the static liquefaction potential under monotonic loading. Two different base gradations of Nevada sand were used. They consisted of gradations between the Nos. 50 and 80 sieve sizes (50/80) (0.300–0.175 mm) and between the Nos. 50 and 200 sieve sizes (50/200) (0.300–0.074 mm). Two different gradations of Ottawa sand were also utilized in the study, and they consisted of sand sieved between the Nos. 50 and 200 sieve sizes (50/200) and Ottawa F-95 sand, which falls between the No. 60 (0.250 mm) and No. 200 sieve sizes. Maximum and minimum void ratios were estimated for four types of soil with varying fine contents. It was found that Nevada 50/80 sand, which is more uniform, shows larger dips in both curves, whereas the Nevada 50/200 sand indicates much flatter curves. The reason for this is that the ratio of mean diameter for the coarse range and the fine range is larger for the 50/80 sand than for the 50/200 sand, allowing the fines to pack more efficiently in the void spaces. Similar observation was seen for Ottawa sand also.

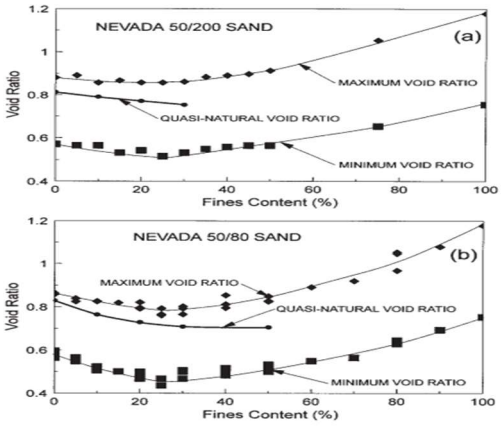

Fig1: Maximum, minimum, and quasi-natural void ratios for variations in fines content on (a) Nevada 50/200 sand, and (b) Nevada 50/80sand. [Lade and Yamamuro (1997)]

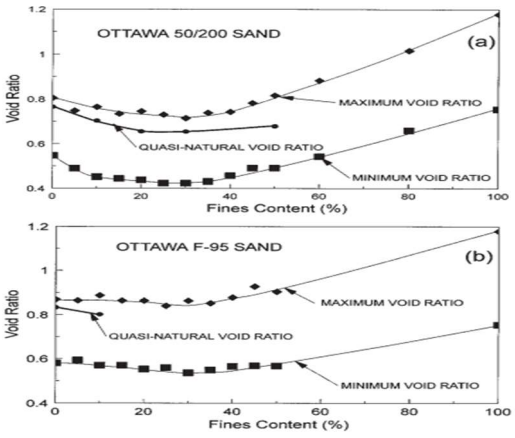

Fig2: Maximum, minimum, and quasi-natural void ratios for variations in fines content on (a) Ottawa 50/200 sand, and (b) Ottawa F-95 sand.[Lade and Yamamuro (1997)]

Specimens from the four different base sands were prepared at their loosest possible densities by the dry funnel deposition method with varying fine content. These specimens were tested for the effect of fines content on the undrained behaviour in triaxial compression. The four different sands had different susceptibilities to liquefaction depending on initial gradation. Clean sands always indicated the highest resistance to liquefaction. All sands showed that increasing the fines content greatly increased the liquefaction potential, even though the relative and absolute densities increase. This observation is inconsistent with normal soil behaviour, which suggests that the soil should exhibit more dilatant behaviour as density increases. This implies that neither relative density nor void ratio may provide satisfactory indications of liquefaction potential in silty sands.

The Nevada 50/200 sand is observed to undergo static liquefaction at all fines contents. Nevada 50/80 sand is also observed to undergo static liquefaction at all fines contents except 0% fine content. At 0% fine content it shows temporary liquefaction. In case of Ottawa sand the response was somehow different. The Ottawa 50/200 sand appears to be more resistant to liquefaction than Nevada sand, since the undrained tests with 0 and 10% fines result in temporary liquefaction type of behaviour. However, as the fines content is further increased, complete static liquefaction ensues.

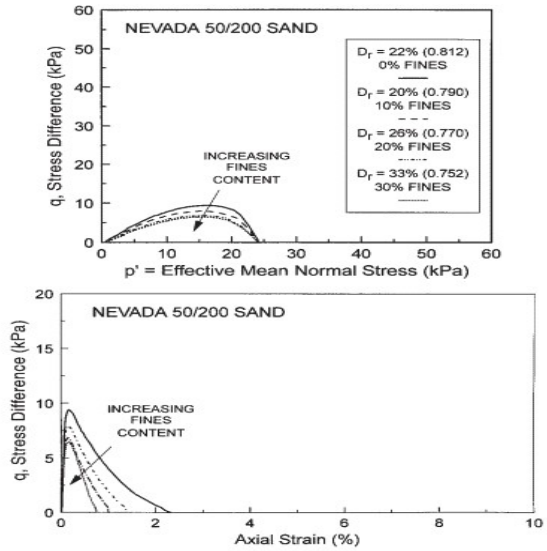

Fig3: Static liquefaction potential increases as fines content and density (Dr) increase on Nevada 50/200 sand at 25 kPa initial confining pressure. (a) Effective stress paths in the p′–q diagram. (b) Stress difference versus axial strain.[Lade and Yamamuro (1997)]

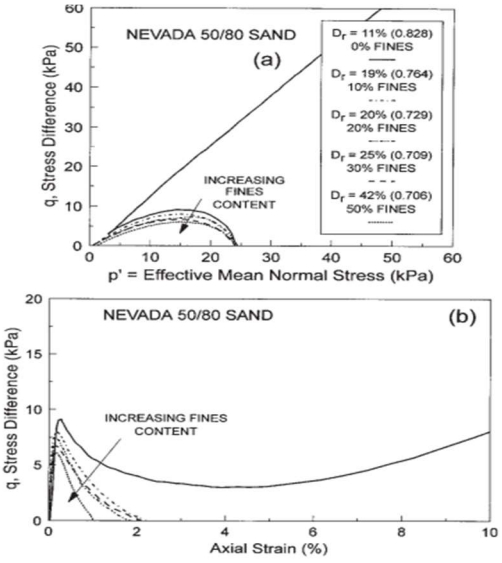

Fig4: Static liquefaction potential increases as fines content and density increase on Nevada 50/80 sand at 25 kPa initial confining pressure. (a) Effective stress paths in the p′–q diagram. (b) Stress difference versus axial strain.[Lade and Yamamuro (1997)]

Polito and Martin II (2001) investigate the effect of silt content on the liquefaction resistance of sand. They conducted cyclic triaxial test on Monterey and Yatesville sand with silt contents varying from 4 to 75%. The specimens tested were 71 mm (2.8 in.) in diameter and 154 mm (6.1 in.) in height. They were formed by moist tamping at a water content that produced 50% saturation in the specimen. To compare the liquefaction potential of silty sand with different initial properties, they defined cyclic resistance as the cyclic stress ratio required to cause initial liquefaction in 15 cycles of loading. Liquefaction potential of different silty-sand were observed at three different conditions i.e. at constant void ratio, constant sand skeleton void ratio, and constant relative density. It was observed by several studies that cyclic resistance is more closely related to sand skeleton void ratio than it is to either void ratio or fines content.

Result obtained shows that for specimens prepared to a constant void ratio, as the silt content increases cyclic resistance first decreases and then increases after some minimum resistance is reached.

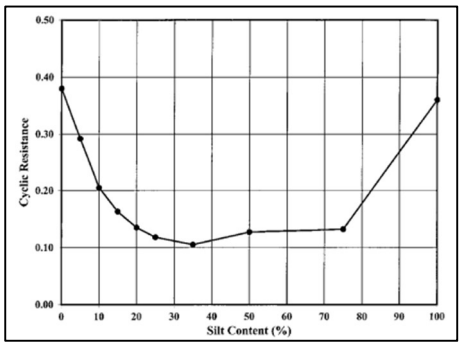

Fig5: Cyclic Resistance of Monterey Sand at Constant Void Ratio with Variation in SiltContent.[Polito and Martin II(2001)]

The effect of altering silt content while holding the sand skeleton void ratio of the specimens constant was examined. Monterey sand was found to maintain a nearly constant cyclic resistance with increasing silt contents (up to Limiting Fine Content) for specimens prepared to a constant sand skeleton void ratio of 0.75.Conversely, below the limiting silt content, Yatesville sand was found to increase in cyclic resistance with increasing silt content for specimens prepared to constant sand skeleton void ratios of 0.9 and 1.0. So, contradictory results has been observed in this case.

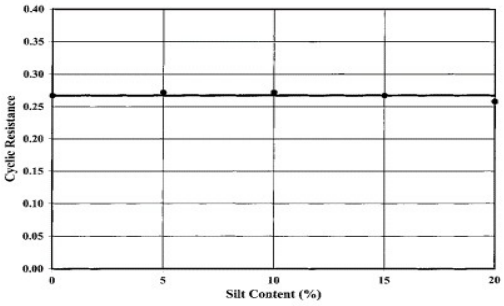

Fig6:Variation in Cyclic Resistance with Silt Content for Specimens Prepared to Constant Sand Skeleton Void Ratio Using Monterey Sand[Polito and Martin II(2001)]

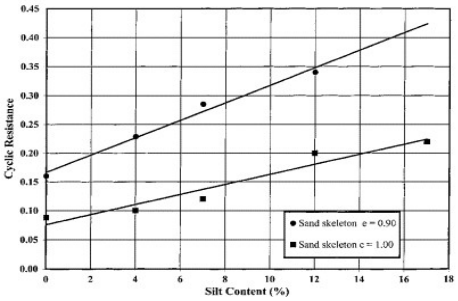

Fig7: Variation of Cyclic Resistance with Silt Content for Yatesville Sand Prepared to Constant Sand Skeleton Void Ratios [Polito and Martin II(2001)]

Cyclic resistance evaluated in terms of relative density shows clear pattern with increase in fine content. At a constant relative density, Cyclic resistance observed to be constant up to LFC and after that it decrease with increase in fine content. On the other hand for specimens with silt contents below the limiting silt content, there is a linear trend between increasing relative density and increasing cyclic resistance. The cyclic resistance of soils above the limiting silt content is also controlled by the relative density of the specimen; however, the cyclic resistance of these soils is markedly lower than it is for soils below the limiting silt content at similar relative densities.

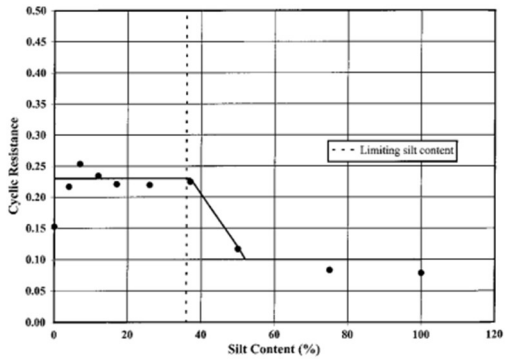

Fig8: Variation in Cyclic Resistance with Silt Content for Yatesville Sand Specimens Prepared by Moist Tamping Adjusted to 30% Relative Density. [Polito and Martin II(2001)]

Xenaki and Athanasopoulos (2003) investigated the effects of fines on Liquefaction resistance of sand. The tests were conducted using cyclic triaxial tests under stress-controlled conditions following the specifications of ASTM D5311. They took six different combination of sand and silt: 100% sand–0% fines, 90% sand– 10% fines, 70% sand–30% fines, 58% sand–42% fines, 45% sand–55% fines and 0% sand–100% fines. The tests were conducted on saturated cylindrical specimens with nominal values of diameter and height equal to 50 and 100 mm, respectively, composed of mixtures of sand (D_{50}= 0.12 mm) and non-plastic (PI = 0) fines having (D_{50} =0.02 mm). All specimens were isotropically consolidated under an effective confining stress equal to σ_3' =200 kPa. The sample preparation was done by oven dried soil, which was subsequently saturated by water flowing from the bottom to the top of the specimen. A very high degree of saturation was achieved in all tested specimens as was verified by the very high values of pore pressure coefficient measured in the tests (B = 0.97–1.0). The time interval required to achieve saturation ranged from 30 min to 5 h, depending on the fines content of the tested soil.

After conducting 61 no of cyclic triaxial tests they observed that, for a constant value of global void ratio, the liquefaction resistance decreases with the addition of non-plastic fines up to a fines content of 44%. Beyond this critical valuethe trend is reversed and the liquefaction resistance increases with increasing fines content. This critical value is observed as threshold value, FC_{th}.

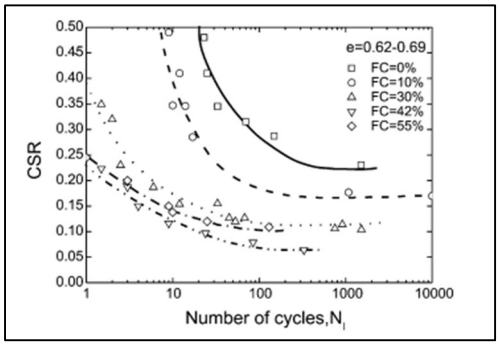

Fig9: Effect of fines content on the liquefaction resistance of sand non-plastic fines mixtures for constant values of global [Xenaki and Athanasopoulos (2003)]

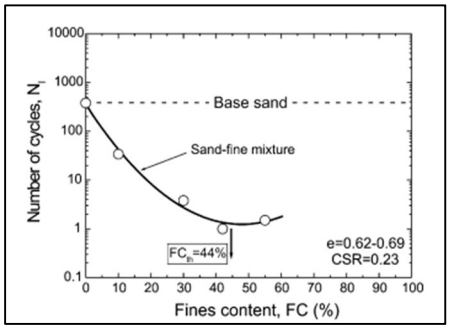

Fig10: Effect of fines content on the liquefaction resistance of sand–non-plastic fines mixtures for constant values of global void ratio and CSR=0:23[Xenaki and Athanasopoulos 2003]

The main mechanism associated with the phenomenon of liquefaction is the generation of excess pore pressure under undrained loading conditions. So, pore pressure generation is an important parameter of this study. They observed that at a constant global void ratio, the rate of pore pressure generation is increased compared to that of sand. It is also noted that the behaviour changes depending on whether the value of fines content is lower or higher than the threshold value, FCth. The behaviour is similar as we see in case of liquefaction resistance.

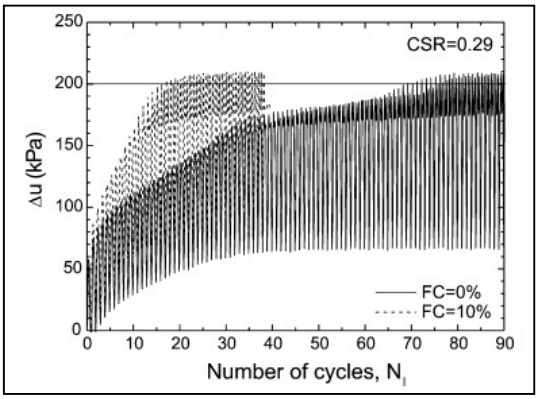

Fig11: Cycles of loading till initial liquefaction with different percentages of non-plastic silt at CSR= 0.10 and constant dry density=13.6 kN/m [Xenaki and Athanasopoulos (2003)]

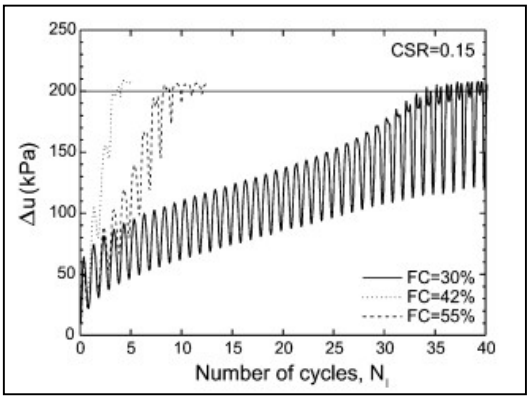

Fig12: Cycles of loading till initial liquefaction with different percentages of non-plastic silt at CSR= 0.10 and constant dry density=13.6 kN/m [Xenaki and Athanasopoulos (2003)]

Naeini and Baziar (2004) studied the effect of silt content on the strength of sandy soil of mixed and layered sample. The study was done by varying silt content from 0-100% using both monotonic and dynamic triaxial test. The samples were prepared by two methods that are Water Sedimentation Method and Under Compaction Method. The specimen was then consolidated isotropically at mean effective pressures between 0.15–0.50 Mpa, and then subjected to undrained monotonic triaxial loading with a constant strain rate of 1% per minute, or undrained dynamic loading at a frequency of 0.1 Hz.

Results obtained shows that as the silt content increase up to 35%, the peak and residual strengths decrease. With further increase in silt content, the peak and residual strengths are increased. However, the strength of silty sand and pure silt is less than the clean sand. The liquefaction behaviour of mixed and layered under compaction samples for different confining pressure is not substantially different. Also, as the confining pressure is increased, the liquefaction potential of silty sands is decreased for both mixed and layered specimens. The results of experimental data also indicate that, in layered samples with the same amount of silt and the same confining pressure as in mixed sample, the peak and residual strengths curves are sited below the strengths of the mixed specimens, but the differences are very little.

Cubrinovski and Rees (2008) conducted a series of monotonic and cyclic triaxial tests on sand with varying fines obtained from Christchurch, New Zealand to evaluate effect of fine content on undrained behaviour of sand. Three types of sample were prepared by varying fine contents by 1%, 10% and 30%. The soil specimen were prepared using the moist-tamping method by firstly preparing the sand to a moisture content of approximately 9%, placing the soil in 6 equal layers, and applying an appropriate amount of tamping for the target specimen density. The samples were isotropically consolidated to an initial mean effective stress of 100 kPa. An axial strain rate of 0.3 %/min was used in strain-controlled monotonic test. The results from monotonic triaxial tests shows that the clean sand mixture has the highest stress at steady state, being close to q = 55kPa, whilst having the lowest relative density of D_r = 5%. The specimen having 30% fine content has the lowest stress at steady state, with q = 5kPa, yet is the densest specimen with a relative density of D_r = 50%. This implies that the addition of fines to the clean sand increased the potential for flow deformation during undrained monotonic loading.

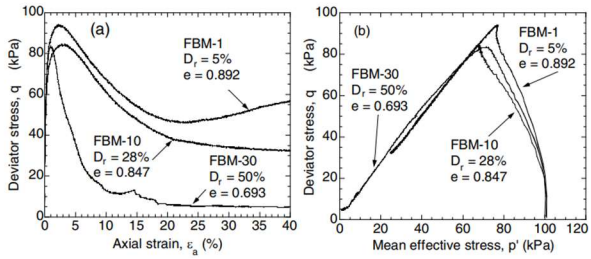

Fig13:Stress-strain curves and effective stress paths observed in monotonic undrained tests on sands with different fines content [Cubrinovski and Rees (2008)]

Cubrinovski and Rees 2008 define the steady state condition of undrained monotonic tests is the sate at 40% strain. The downward shift in the steady-state line with increasing fines content in effect implies that fines tend to increase the flow potential and make the sand more contractive during undrained monotonic loading, at least when the relative density is used as a basis for comparison.

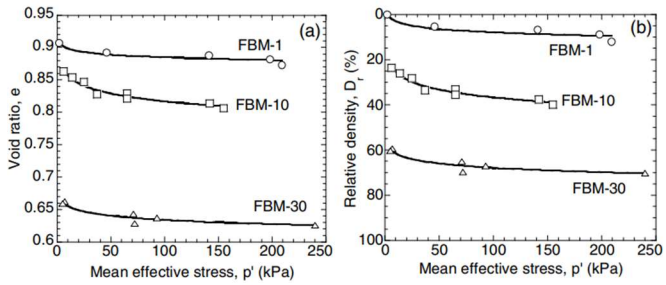

Fig14: Effects of fines on the position of the steady-state line: (a) e-p' plane; (b) Dr-p' plan [Cubrinovski and Rees (2008)]

Undrained cyclic triaxial tests were performed on the same soil specimen to assess the liquefaction potential of the soil with fines. Results obtained clearly shows that at any relative density the clean sand shows higher cyclic strength than the sand containing 10% or 30%

fines. In other words, the liquefaction resistance of soils decreases with increasing fines content at a constant relative density.

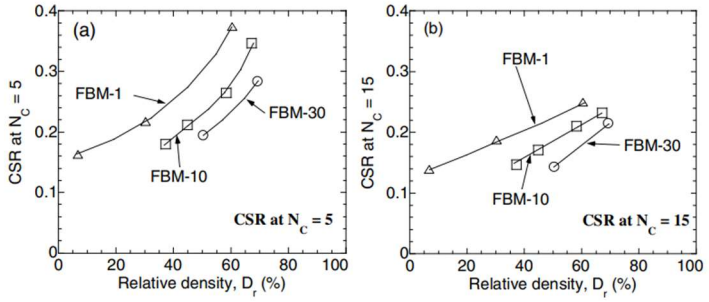

Fig15: Cyclic stress ratio required to cause 5% DA strain in 5 cycles (a) and 15 cycles (b) as a function of relative density [Cubrinovski and Rees (2008)]

Juneja and Raghunandan (2010) studied the effect of sample preparation on stress-strain behaviour of sand. They prepared sand samples by four techniques. These are two types of tamping methods (i.e. Dry tamping and Wet tamping) and two types of pluviation methods (i.e. Dry pluviation and Wet pluviation) with void ratio varies from 0.603 to 0.687. Both Drained and undrainedtriaxial test were conducted on these sample of varying void ratios prepared using different sampling methods. After extensive study, they concluded that samples prepared using tamping technique usually strain softens, whilst samples prepared by pluviation technique may harden or soften with strain depending up on the sample relative density and confining pressures.

Usmani et al. (2011) conduct strain controlled triaxial test on Delhi Silt to find out its properties. Both CD and CU tests are performed to determine the drained and undrained behaviour of soil under tested. The sand used in the study was fine sand whose particle size lies in the range of 425–75 μm. The specific gravity (G_s) of pure silt and fine sand are 2.72 and 2.66 respectively. Two representative ratios of Delhi silt consisting of 40% and 80% silt, along with fine sand, were taken for the preparation of remoulded saturated samples. Slurry deposition technique in the laboratory is adopted to prepare the sample.

The soil compositions used in the study are S60M40 and S20M80, where S stands for sand, M for silt, and numbers representing their percentages. Specific gravity (Gs) of the two soils S60M40 and S20M80 were determined as 2.68 and 2.72, respectively and the void ratio e for S60M40 and S20M80 were 0.64 and 0.69, respectively. All the tests were conducted at a dry density of 16.2 kN/m3, which is a typical value encountered in the Delhi region. The strain rates adopted for testing are 0.1%/min and 0.02%/min for S60M40 and S20M80 soils, respectively, for drained conditions. The strain rates adopted for testing were 0.4%/min. and 0.2%/min for S60M40 and S20M80 soils, respectively, for undrained conditions. A series of conventional triaxial test were performed under four confining pressure of 100, 150, 200, and 300 kPa.

Drained Stress-Strain Behaviour

Results obtained from tests showed that peak stress is reached for S60M40 (silty sand) at all the confining pressures. S20M80 (sandy silt) exhibited stress-hardening behaviour for the entire range of confining pressures, and the rate of increase of deviator stress decreased with the increase of strain. Dilative behaviour of S60M40increased with increasing confining pressure. In contrast, S20M80 did not exhibit any dilative behaviour, due to a higher percentage of fines, i.e., silt, in the soil. Volumetric strain was found to increase with axial strain under all confining pressures.

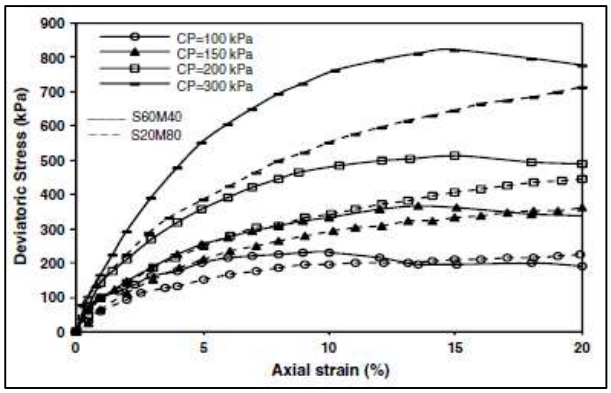

Fig. 16 : Drained stress-strain response of S60M40 and S20M80 soil [Usmani et al. (2011)]

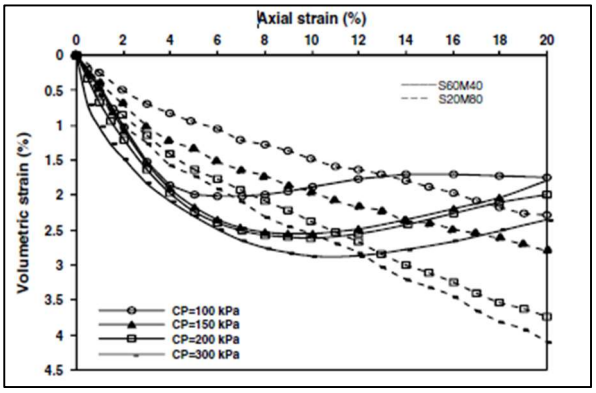

Fig.17 : Volumetric change behaviour of S60M40 and S20M80 soil [Usmani et al. (2011)]

Undrained Stress-Strain Behaviour

The deviatoric stress is found to increase with increasing confining pressure for both soils, with a higher rate of increase observed for S60M40 soil. This stress increase was found to be steeper for higher confining pressures. In the case of S20M80 soil, the deviatoric stress for soil increases sharply during lower strain values of up to 4% and, thereafter, gradually as strain values move toward 20%.

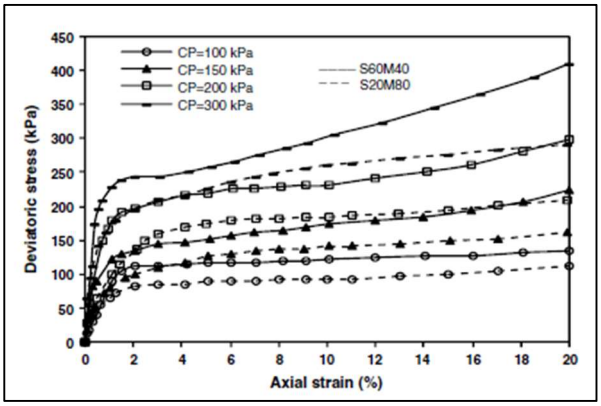

Fig.18 :Undrained stress-strain response of S60M40 and S20M80 soils [Usmani et al.(2011)]

Sachan (2011) presented the soil test data obtained is a function of boundary condition of triaxial setup. For past several decades, triaxial testing has been a common practice across the world to obtain the shear strength parameters of soils. However, the boundary conditions provided to the soil specimen in a triaxial test could not have been still simulated with the

boundary conditions of the soil at site. So, is an important task of a geotechnical engineer to simulate the actual field condition while obtaining data from a triaxial test.

This research is focused on the effect of boundary conditions of triaxial testing and its associated drainage conditions on the obtained shear testing data for a given soil. Three series of triaxial undrained compression tests were performed on Kaolin clay specimens for three different boundary systems: a) Conventional boundary, b) Advanced Frictional end boundary, and c) Lubricated end boundary. The obtained experimental results for various boundary conditions reported that the Lubricated end boundary system had potential to simulate with the boundary conditions of soil at site, which possessed almost no friction at specimen's ends in the soil site. Therefore, Lubricated end boundary system was chosen for further evaluation to assess the proper drainage arrangement in the system in order to acquire the complete pore pressure dissipation throughout the triaxial test. Three different drainage conditions in Lubricated end boundary triaxial system were prepared based on its filter paper arrangements on radial drainage strip of each platen, which were further examined by performing a series of drained triaxial compression tests on Kaolin clay specimens. The key observations are noted from this study are:

- A marked increase in excess pore pressure evolution was observed as the friction at the boundary got reduced due to almost no friction at the specimen's ends in lubricated end boundary system.
- The effective friction angle was observed to be 4-5 deg higher for lubricated end boundary as compared to the other two boundary systems indicating the strong impact of specimen's boundary conditions on its shear strength response.
- The shear strength of soil was found to be twice for Good drainage conditions as compared to the Poor drainage conditions.
- A difference of 8° in φ' values of soil was observed for poor and good drainage conditions exhibiting the importance of appropriate drainage conditions in a triaxial equipment facilitated with lubricated end boundary system.

Muley et al. (2012) examined the effect of fines on liquefaction resistance of Sand obtained from Solani river bed near Roorkee. Experiment conducted on sand classified as Poorly Graded sand (SP) and silt as low plasticity silt (ML).Strain controlled cyclic triaxial test were performed according to ASTM 3999-11, on Solani sand with different percentages of silt content (0%, 5%, 10%, 15% & 20%), at 2 relative densities 35% & 50% at constant effective confining pressures of 50 kPa and frequency of 1 Hz. In this study adopted a strain approach because excess pore water pressure generation is controlled mainly by the level of induced shear strains. Maximum shear strain level was 0.75%.

After performing 10 no of test it was observed that increase in percentage of non plastic silt in pure sand increases liquefaction resistance of sand. The optimum value of silt contents for 35% and 50% relative densities were found to be 15% and 10%, respectively. The number of cycles for liquefaction for the same value of silt content increases when the relative density is

increased. Thus, relative density still plays a role but at higher fine contents, its effect decreases.

Belkhatir et al. (2012) conducted a series of undrained monotonic triaxial tests on reconstituted saturated silty sand samples with different fines content ranging from 0 to 50 % at two initial relative densities (D_r = 20 and 91 %). Their findings aims to evaluate the effects of low plastic fines, gross void ratio, intergranular void ratio, relative density and gradation characteristics on the saturated undrained shear strength (liquefaction resistance) response of silty sand samples. The variation of $e_{max}$and e_{min} versus the fines content F_c (the ratio of the weight of silt to the total weight of the sand-silt mixture) shows that as the fine content increases both the void ratios decreases up to a value of 30% fine content, after further increase in fine content both the void ratios increases. This particular fine content can be known as Limiting Fine Content (LFC).

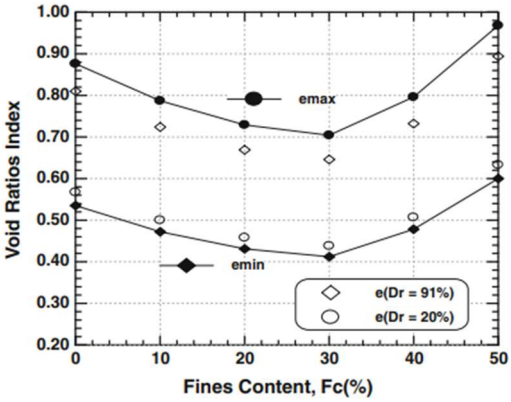

Fig 19: Void ratios index of the sand-silt mixtures versus fines content (σ_3'= 100 kPa) [Belkhatir et al. (2012)]

They conducted all undrained triaxial tests out at a constant strain rate of 0.167 % per minute, which was slow enough to allow pore pressure change to equalize throughout the sample with the pore pressure measured at the base of sample. All the tests were continued up to 24 % axial strain. Their study shows that the initial global void ratio (e) decreases almost linearly with the decrease of the effective diameter and increase of the fines content until the value of 30 % and then it increases significantly with the decrease of the effective diameter and increase of the fines content. Nearly Similar observation was made for mean grain size (D_{50}) and coefficient of uniformity (C_u).

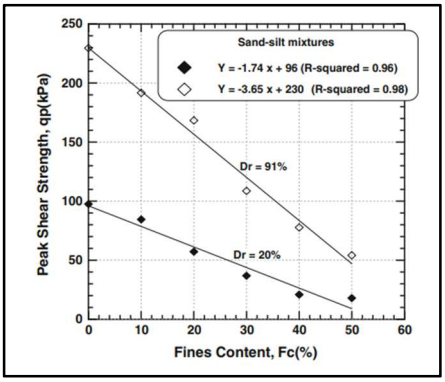

Fig20: Peak strength versus fines content at various initial relative densities σ_3'= 100 kPa) [Belkhatir et al. (2012)]

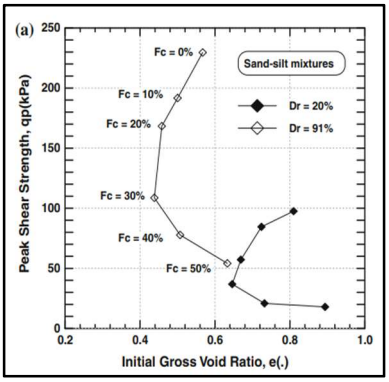

Fig21: Variation of the peak strength with the initial gross void ratio and fines content (σ_3'= 100 kPa) [Belkhatir et al. (2012)]

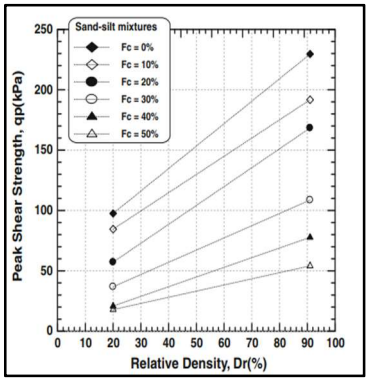

Fig22: Peak strength versus initial relative density at various fines contents (σ_3'= 100 kPa [Belkhatir et al. (2012)]

From the results of undrained triaxial tests, they observed that the increase of the low plastic fines induces a decrease of the sand-silt mixture liquefaction resistance. This decrease results isdue to the role of the fines to increase the contractiveness of the sand-silt mixtures leading to an increase of the excess pore pressure and consequently to a decrease of the peak resistance of the mixtures as shown in the figure below.

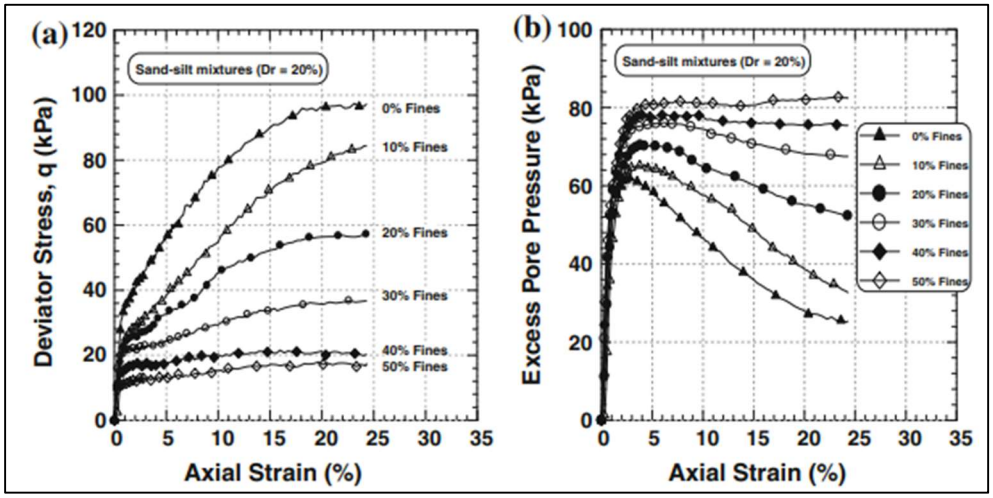

Fig23: Undrained monotonic response of the sand-silt mixtures (σ_3'= 100 kPa, Dr = 20 %) [Belkhatir et al. (2012)]

They also observed that peak undrained shear strength (q_{peak}) of the sand-silt mixtures decreases linearly with the increase of the fines content and converges towards a unique value of the peak strength for higher fines content for the two initial relative densities (D_r = 20 and 91 %). The peak undrained shear strength (q_{peak}) decreases logarithmically as the intergranular void ratio (e_s) increases. It is also clear from their study that an increase in the relative density results in an increase in the peak strength at a given fines content.

It can be seen from the study that the normalized undrained residual shear strength (S_{us} /σ_3') of the sand-silt mixtures decreases linearly with the increase of the fines content for the tinitial relative densities (Dr = 20 and 91 %).

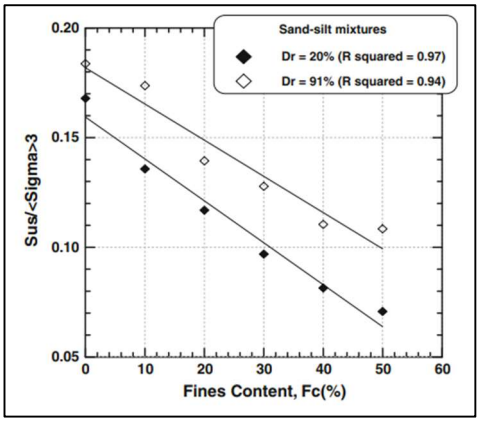

Fig24: Normalized residual strength versus fines content σ_3'= 100 kPa [Belkhatir et al. (2012)]

Alam et al. (2013) conducted stress-controlled cyclic triaxial test on silty sand to find out effect of fine content on dynamic properties and liquefaction potential of a sandy Soil. Soil specimens of size 71 mm diameter and 143 mm in height were prepared using wet tamping

technique. The sand was initially mixed in a container with 8% to 10% moisture. Then the wet sand was poured into the mould in 5 layers and compacted in 5 layers using 35.5 mm diameter circular aluminium tamper, weighing about 800 g at a relative density of 55%.The cyclic triaxial strength tests were conducted under undrained conditions to simulate essentially undrained field conditions during an earthquake or dynamic loading. The tests were conducted at a constant Cyclic Stress Ratio (CSR = ($\sigma_{dc}/2\sigma_c'$, where σ_{dc}= cyclic deviator stress and σ_c'= effective confining pressure). CSR was varied from 0.15 to 0.45 at the interval of 0.05. In the entire test program, a harmonic loading was applied using sine wave with a frequency of 1 Hz, the maximum peak-peak axial strain 10%, the number of cycles limited to 100 cycles and a recording speed of 50 numbers of readings per cycle was specified. Axial deformation, cell pressure, cyclic load, and sample pore water pressure were recorded using automatic data acquisition system. They observed that under a constant cyclic vertical load application the pore pressure increases gradually until cycle 21 where the excess pore water pressure just equal to the effective confining pressure, which is defined as initial liquefaction. In addition, it is mentioned that small cyclic deformations were induced in the specimen until approximately cycle 19, after which the cyclic deformations built up rapidly.

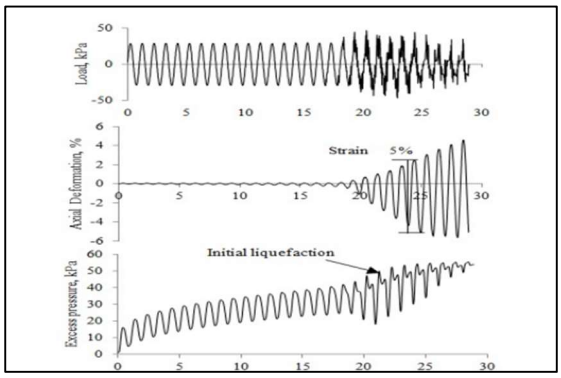

Fig25: Recorded load, deformation and pore water pressure time history for cyclic stress ratio 0.30 [Alam et al. (2013)]

It is also observed that the number of cycle required to failure decreases with increasing cyclic stress ratio. Initial liquefaction occurred before the 5% DA axial strain in all tests. The cyclic strength of the soil is specified in terms of magnitude of cyclic stress ratio (CSR) required reaching 5% double amplitude axial strain in 20 cycles of uniform load application, and the cyclic strength ratio of the sand is 0.315.

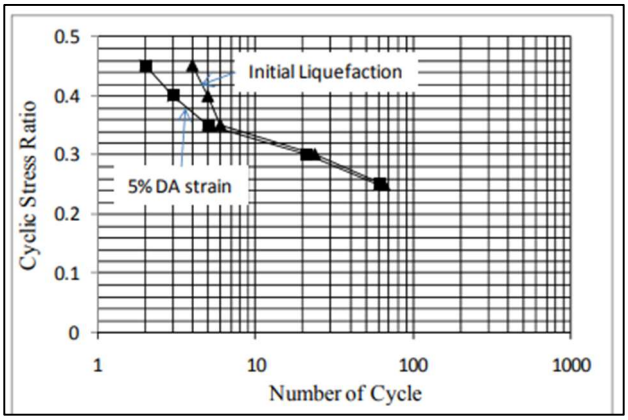

Fig26: Variation of cyclic stress ratio with the number of cycles [Alam et al. (2013)]

Kirar and Maheshwari (2013) conducted cyclic triaxial tests on Solani sand, collected from the bed of Solani River near Roorkee. The effects of silt content on shear modulus of Solani sand at different shear strain are evaluated. Strain controlled cyclic triaxial test were performed according to ASTM 3999-11, on Solani sand with different percentages of silt content (0%, 5%, 10%, 15% & 20%), at 2 relative densities 35% & 50% at constant effective confining pressures of 50 kPa and frequency of 1 Hz. Axial strain on which samples were tested was 0.75%. Shear modulus at different strain levels have been determined and compared with that of sand specimen. The samples were prepared using water sedimentation method. The quantity sand required for specific relative density was calculated using standard co-relations and silt is added to it as % of sand required. Tests were conducted at different relative density and following observations were made:

- As the shear strain increases shear modulus (G) and modulus ratio (G/G_{max}) decreases. For any specific relative density maximum modulus ratio (G/G_{max}) is found at 10% silt content.

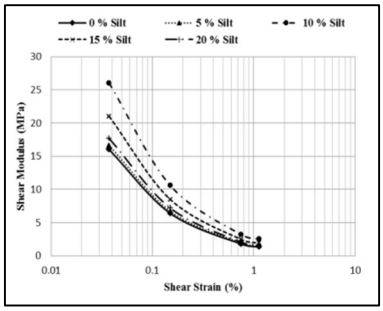

Fig.27 : Influence of silt content on shear modulus versus shear strain at 35 % [Kirar and Maheshwari (2013)]

- The % increase (w.r.t. pure sand) in shear modulus is increasing with increase in shear strain. It can be observed that maximum increase in shear modulus values is for 10% silt content at all shear strains.At 1.125% shear stain, % gain in G value is as high as 90% for 10% silt content which is quite remarkable.
- In case of damping ratio first it decrease and then it increase with increase in silt content. Damping ratio is minimum at 10% silt content.
- So, 10% silt content is found to be optimum silt content at which shear modulus ratio is maximum while damping ratio is minimum.

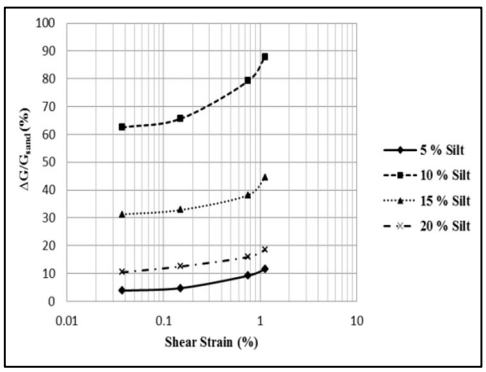

Fig.28: Percent increase in shear modulus with silt content at different shear strains at 35% RD [Kirar and Maheshwari (2013)]

- Effect of relative density on sand mixed with silt is similar to that on sand i.e. with relative density shear modulus increases while damping ratio decreases.

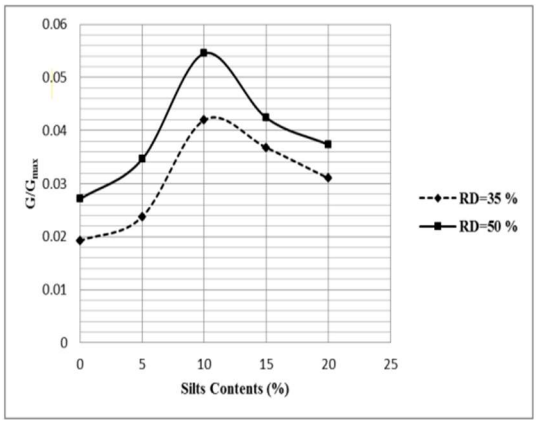

Fig. 29: Influence of relative density on normalized shear modulus versus silt contents at 1.125 % shear strain [Kirar and Maheshwari (2013)]

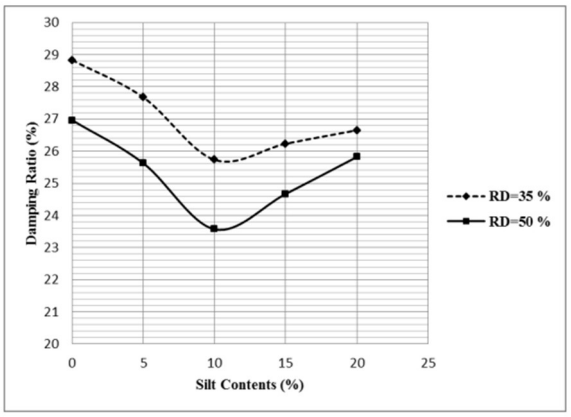

Fig. 30: Influence of relative density on damping ratio versus silt contents at 1.125 % shear strain [Kirar and Maheshwari (2013)]

Kumar et al. (2014) used Brahmaputra sand for determination of dynamic properties of soil using stain controlled Cyclic Triaxial tests. The soil used is classified as poorly graded sand (SP) of Specific gravity 2.7 and the maximum and minimum dry densities are obtained as 16.841 kN/m3 and 13.849 kN/m3 respectively. A series of strain-controlled undrained tests have been conducted on samples at relative density 60% and at peak axial strain 0.01% - 3% subjected to varying confining pressures (50 kPa, 100 kPa and 150 kPa) and loading frequencies (0.1 Hz, 0.5 Hz, 1 Hz, 2 Hz, 3Hz and 4 Hz).Based on the experiment results it is observed that the dynamic soil properties, as obtained from the first loading cycle, are strongly influenced by confining pressure and shear strain. High shear strains (γ>1%) has been found to produce a quasi-liquefaction state manifested by the rise of first-cycle peak excess pore-water pressure ratio near to or greater than 1 (one), which results in a decrease in the damping ratio. For a particular shear strain, an optimum loading frequency has been observed (f~2Hz) beyond which the dynamic response of the soil is substantially affected.

Hsiao and Phan 2014 investigate the static and dynamic properties of sand-silt mixtures using static triaxial, cyclic triaxial and resonant column tests. Tests were conducted on various sand-silt mixtures with three types of specimens, i.e., a constant void ratio of 0.582 (type A), the same peak deviator stress of 290 kPa with a confining pressure of 100 kPa (type B), and a constant relative density D_r of 30% (type C) to understand the effects of low-plastic

silt content on the results of the angle of internal friction and cohesion, the liquefaction resistance, and the shear modulus and damping ratio of sand-silt mixtures. Also tests were conducted with four sand-silt mixtures defined by dry weight: 100% sand plus 0% silt (sample 1), 85% sand plus 15% silt (sample 2), 70% sand plus 30% silt (sample 3), and 50% sand plus 50% silt (sample 4) under each type of specimen A, B, C. Maximum and minimum void ratios were determined for four different types of sand-silt mixtures. It was seen that both the maximum and minimum void ratio of sand-silt mixtures is initially reduced with an increase in silt content until it reaches a minimum value at a limited silt content of 18% and continuously increases with further increases in the silt content.

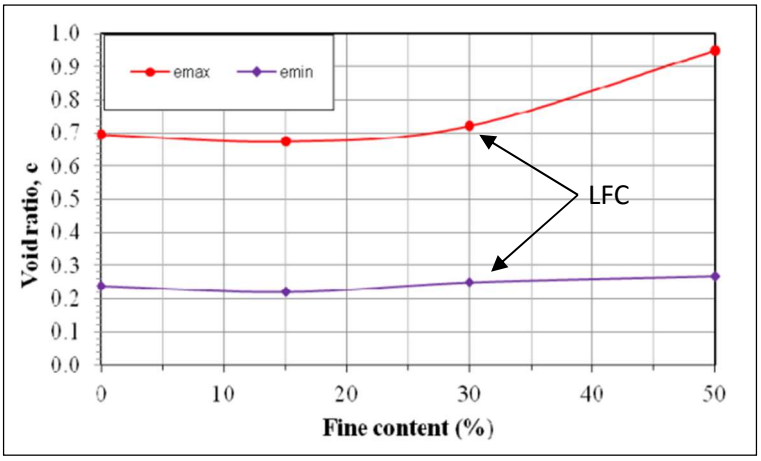

Fig.31: Variation of the void ratio index with different silt contents in the sand-silt mixtures [Hsiao and Phan 2014]

The diameter and height of the specimens were 7.1 cm and 15 cm, respectively, for static and cyclic triaxial testing and resonant column testing. The specimens were prepared using the wet tamping method. The effective consolidation pressure was fixed at 100 kPa for each sample. Static triaxial testing was conducted in both the consolidated-drained and consolidated-undrained stage using a static triaxial testing device that was automatically controlled using hydraulic lifting equipment and collected measured data with a digital display monitor. Confining pressures of 50, 100, and 200 kPa were applied in all tests. The cyclic triaxial tests were conducted in accordance with ASTM D5311 using the automatic triaxial testing system. The variations in excess pore water pressure, axial stress, and axial strain of the specimens were recorded during cyclic loading. The frequency of cyclic loading was fixed at 1 Hz. A series of cyclic triaxial tests were conducted on various sand-silt mixtures with silt contents from 0 to 50% at a 100-kPa effective confining pressure to determine the liquefaction resistance.

Results of static triaxial tests

Both CU and CD tests were conducted in static triaxial test. For the consolidated drained test, the greater the silt content in the sand-silt mixture, the smaller the angle of internal friction becomes, and thus the cohesion is greater. The main reason for this observation is that in the drained shear environment, the low-plastic silt particles not only mobilize the cohesive strength but also take advantage of the slipping between aggregate particles. In contrast, as the silt content increases, both the cohesion and internal friction angle decrease when the consolidated undrained triaxial test is conducted on type A. These behaviours most likely

occur because the low-plastic particles are difficult to mobilize the cohesive strength in the mixture with the presence of pore water pressure; moreover, the low-plastic particles also contribute to the easy slip between the aggregate particles in the undrained shear environment.

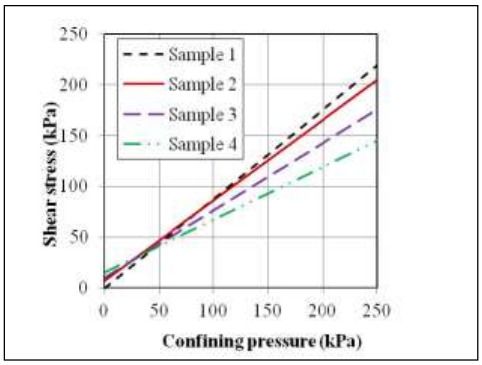

Fig.32: Consolidated drained - Type A [Hsiao and Phan 2014]

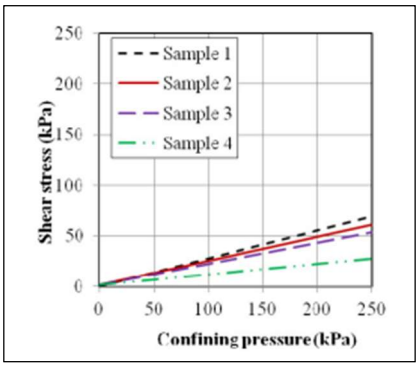

Fig.33: Consolidated undrained - Type A [Hsiao and Phan 2014]

They also observed the relationships of deviator stress, volumetric strain, and pore water pressure (PWP) versus axial strain in the consolidated drained and consolidated undrained triaxial tests. It was observed from the study that that as the silt content increases; the peak deviator stress is decreased corresponding to the axial strain range of 12% and 17%. Furthermore, it is noted that an increase in the amount of silt particles requires a longer time duration to reach the same deviator stress, and the volumetric strain decreases with the increase in silt content in case of CD test. These behaviours most likely occur because as the sand-silt mixture includes additional silt particles, the friction of the mixture remarkably decreases in the consolidated drained shear test. In case of CU test it was seen that the deviator stresses quickly reach the peak value with an axial strain in the range of 0.5 and 2%, and thereafter, drop significantly in value with the increase in axial strain. The pore water pressure (PWP) of all sand-silt mixtures rapidly increases as the axial strain reaches 1-2%, and afterward, the PWP slowly increases and reaches a stable state with a strain of 5% and 6%; however, the PWP of clean sand increases more slowly than that of the sand-silt mixtures.

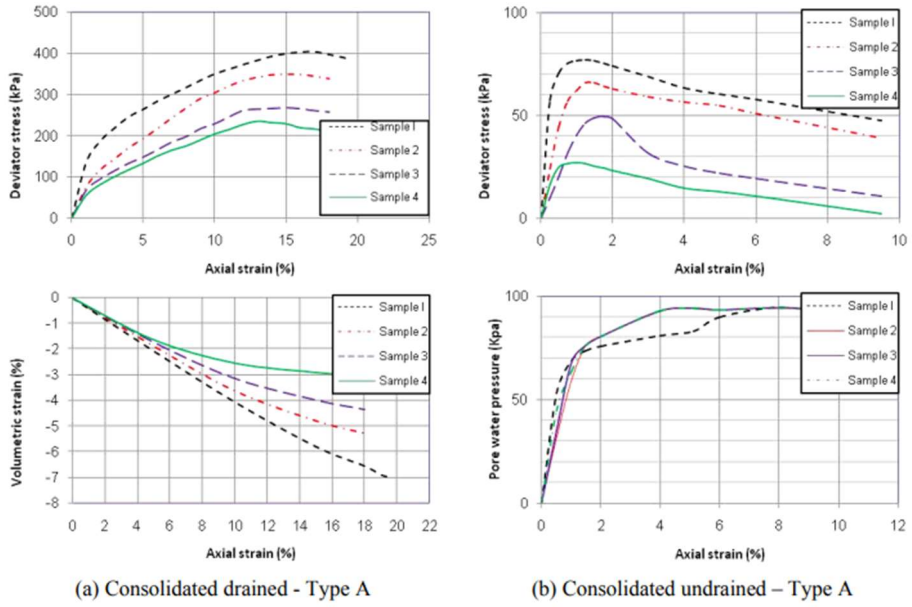

Fig.34: (a) Deviator stress and volume change; (b) Deviator stress and pore water pressure at a confining pressure of 100 kPa [Hsiao and Phan 2014]

Results of cyclic triaxial tests

The cyclic triaxial test was conducted on various sand-silt mixtures with three types of specimens, i.e., type A, type B, and type C, and the effect of substituting silt content in the cyclic stress ratio of the mixture was observed. To estimate the liquefaction resistance of specimens with an earthquake of magnitude 7.5, the liquefaction resistance is defined as the cyclic stress ratio required to cause initial liquefaction within 15 cycles of loading. In case of type A specimen, the greater the silt content in the mixture, the smaller the CSR obtained. In case of type C sample, the CSR gradually decreases with the increase in silt content from 0% to 15%, and afterwards, the value significantly decreases with further increases in silt content to 30%. The result from the specimen with 50% silt content was not obtained due to a weak sample. In case of B type specimen, increases in the silt content will decrease the CSR of the sand-silt mixture until the silt content approaches the limit value of 30%. Furthermore, as the silt content increases to greater than 30%, the CSR increases.

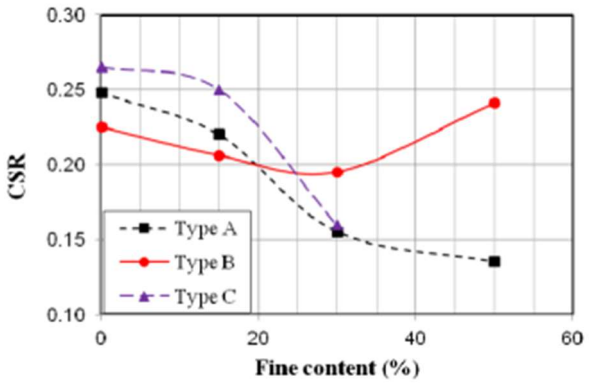

Fig.35: Cyclic stress ratio versus silt content [Hsiao and Phan 2014]

They also tried to give a relationship between internal friction angle and CSR which contribute to an understanding of the relationship between the static and dynamic properties of sandy soil containing different silt contents in the study area. The observation shows that with an increase in the internal friction angle in the sand-silt mixture, the cyclic stress ratio generally increases.

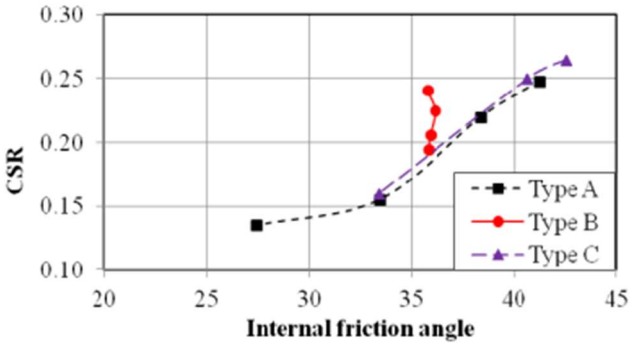

Fig.36: Relationship between internal friction angle and CSR [Hsiao and Phan 2014]

Kumar (2014) discussed the parameter influencing dynamic soil properties. Dynamic soil properties namely shear wave velocity, variation of stiffness or modulus reduction and material damping with strain levels, and liquefaction susceptible parameters are the primary input parameters for various dynamic studies and investigations. So, the determination of dynamic soil properties is an utmost critical and important aspect of geotechnical earthquake engineering problems. It has been observed that dynamic properties of soils are affected by many factors like: method of sample preparation in laboratory (intact and reconstituted samples), relative density, confining pressure, methods of loading, overconsolidation ratio, loading frequency, soil plasticity, percentage of fines and soil type. Effect of these parameters is mention below:

- The method of sample preparation influences the dynamic soil properties. There are many methods for sample preparation as suggested by different researchers like air-pluviation, wet-tamping, moist-vibration, trimming, spooning and raining technique. The weakest (loose) specimens were formed by air-pluviation technique, while strongest (dense) formed moist-vibration technique. Damping ratios were not significantly affected by methods of sample preparation while the effect on the shear modulus was significant.
- Shear modulus, damping ratio and liquefaction are significantly influenced by confining pressure. As the confining pressure increases, the shear modulus increases and damping ratio decreases. Subjected to higher confining pressure, the number of loading cycles required for liquefaction increases.
- Densification or reduction in void ratio of soils due to confining pressure and method of sample preparation lead to increase cyclic strength.

- Cyclic loading or excitation waveform affects the dynamic response of the specimen. Sinusoidal waveform loading gives approximately 30% higher cyclic strength than the rectangular or triangular waveforms.
- Frequency of cyclic loading does not significantly affect the shear modulus, although there is a significant influence on the damping ratio.
- Shear modulus, damping ratio and liquefaction parameters are also significantly affected by the quantity of plastic and non-plastic fines/silts present in the specimen.

Karim and Alam (2014) conducted stress-controlled triaxial test to determine the effect of non-plastic silt on the cyclic behaviour of sand–silt mixtures. Fine sand and silt were collected from sandbars of Padma River, Mawa, Bangladesh, near the proposed Padma Bridge site. They mixed sand with varying silt content ranges from 0-100%. They used two methods i.e. Constant dry density approach and Constant relative density approach to observe the effect of silt content on different parameters such as liquefaction potential, pore pressure generation, cyclic shear modulus etc. The following observations were made after conducting the study:

- At a constant dry density of 13.6 kN/m^3 and CSR= 0.10, it is observed that the liquefaction potential of the sand sample increases with increase of non-plastic fines up to 30% (till limiting silt content). However, with further increase in non-plastic fines (FC>30%) the liquefaction potential is found to be decreasing. They also observed that in constant relative density approach the cyclic resistance decreases rapidly till around the limiting silt content and beyond limiting silt content it remains relatively same for all the silt contents till pure silt.

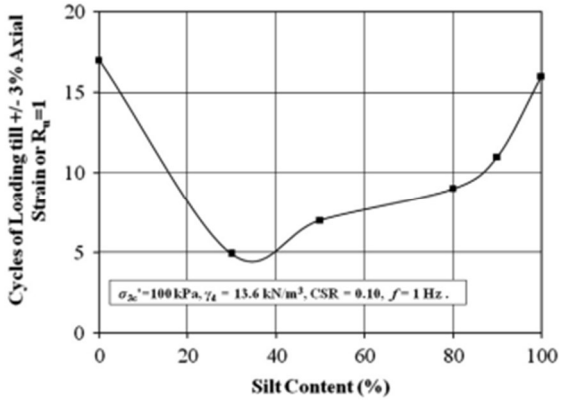

Fig.37: Cycles of loading till initial liquefaction with different percentages of nonplastic silt at CSR= 0.10 and constant dry density=13.6 kN/m [Karim and Alam (2014)]

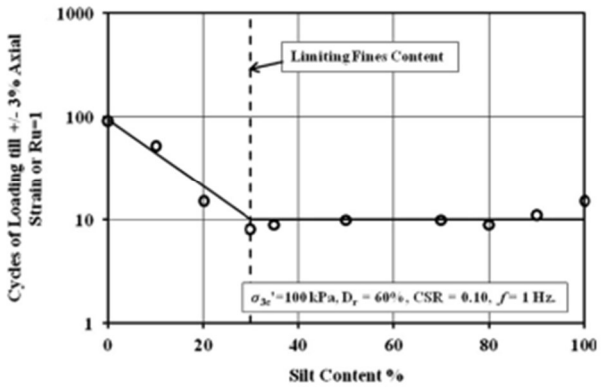

Fig.38: Cycles of loading till Ru=1 or 3% axial strain versus silt content at Dr=60% and CSR=0.10. [Karim and Alam (2014)]

- They observed that pore pressure ratio increases with increase in percentage of non-plastic fines (FC<30%). With further increase in non-plastic fines (FC>30%) excess pore pressure ratio decreased. In addition, number of cycles for initial liquefaction decreases with increase in the percentage of non-plastic fines content (FC<30%). However, with

further increase in the non-plastic fines (FC>30%) the number of cycles for initial liquefaction has been found to increase.

- Cyclic resistance Ratio (CRR) of sand–silt mixture of desired silt content and relative density 60% was determined as CSR at which liquefaction occurred for 15 cycles of loading. Up to LFC, CRR decreased; after that CRR remained constant.
- It was observed that with increasing silt content the secant shear modulus (G_{sec}) decreases till LFC=30%; after LFC G_{sec} became constant.

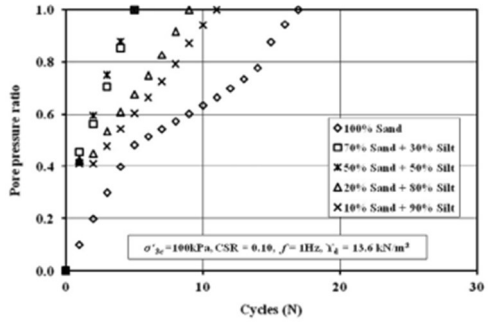

Fig.39: Effect of relative density on the pore pressure generation with number of loading cycles for clean sand at CSR=0.10. [Karim and Alam (2014)]

Kumar et al. (2015) conducted stress-controlled cyclic triaxial test on Brahmaputra river-bed sand collected at Guwahati. The sand used in the experiment is classified as poorly graded sand (SP). Samples prepared at 60% relative density were subjected to cyclic stress ratios (CSR) in the range of 0.1-0.4 at a loading frequency of 1Hz and under confining pressures of 100 kPa. The test results reveal that CSR and number of cycles (N) significantly influence the development of excess pore water pressure and the associated dynamic soil properties. It was observed that the shear modulus estimated from each cycles with accumulated shear strain portrayed conventional degradation pattern (Fig. 11a) with the increase in shear strain corresponding to CSR, while the damping ratio exhibited non-conventional degradation pattern beyond a shear strain of 0.75% (Fig. 11b), primarily due to the first cycle quasi-liquefaction state attained by the strained sample.

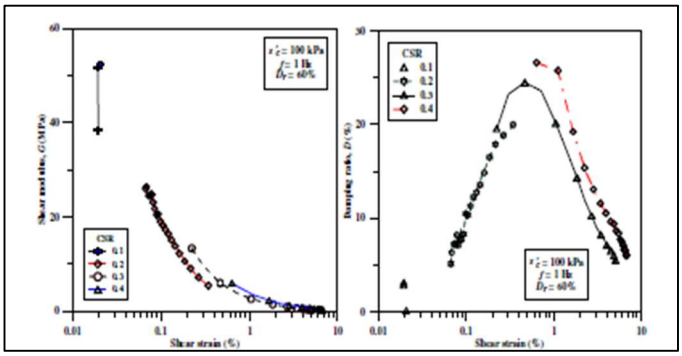

Fig.40: Variation of dynamic properties of Brahmaputra sand for varying CSR and shear strain (a) Variation of dynamic modulus (b) Variation of damping ratio

[Kumar et al. (2015)]

Banupriya et al. (2015) examined Stress-Strain and Strength Characteristics of Sand-Silt Mixtures by conducting strain controlled triaxial test. Sand used in the study was poorly graded sand (SP) with Coefficient of uniformity, Cu = 3.57, Coefficient of curvature, Cc = 1.201 and specific gravity 2.62. The specific gravity of non-plastic silt was 2.72. Samples were prepared by mixing sand and silt with proportion of silt ranges from 10-100 % of dry weight of soil. To find the stress-strain characteristics of sand and sand-silt mixtures, a series of triaxial tests was performed on sand and sand-silt mixtures in dry state with the confining pressure of 50 kPa to 250 kPa at a strain rate of 0.12mm/min. The density at which test conducted was 1.47g/cc. A typical result from triaxial test performed at 100 kPa confining pressure is shown below :

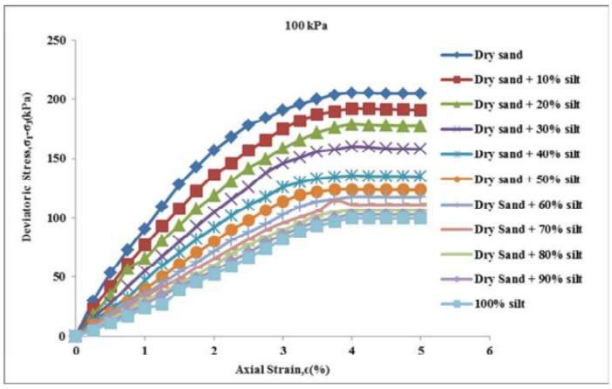

Fig.41: Stress-strain curve of sand-silt mixtures for confining pressure of 100 kPa [Banupriya et al. (2015)]

After analysing all the test result they observed the followings:

1. Irrespective of grain size (i.e., for sand, sand-silt mixtures and non-plastic silt) increases in confining pressure increased the failure deviatoric stress and failure axial strain. And increasing in the silt content decreases the failure deviatoric stress for all the confining pressures.

2. The angle of internal friction decreases with increases in the silt content from 10 to 100% to the sand. The difference in the angle of internal friction of 10-40% of non-plastic silt content the reduction is more when compare to the other proportion of 50-100% of non-plastic silt content.

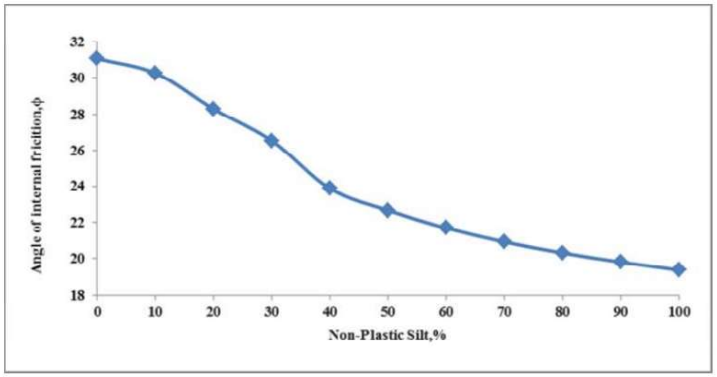

Fig. 42 : Effect of non-plastic silt content in angle of internal friction of sand[Banupriya et al. (2015)]

3. The intergranular void ratio (e_s) increases with the increase of the non-plastic fines content. And it has been seen that intergranular void ratio is greater than maximum void ratio of clean sand when the non-plastic fines content is increasing beyond 10%. It means that the sand particles are on average, not in contact and mechanical behaviour is no longer controlled by the sand matrix. The angle of internal friction decreases as the intergranular void ratio increases. It means that when increasing in the fines contents the angle of internal friction decreases.

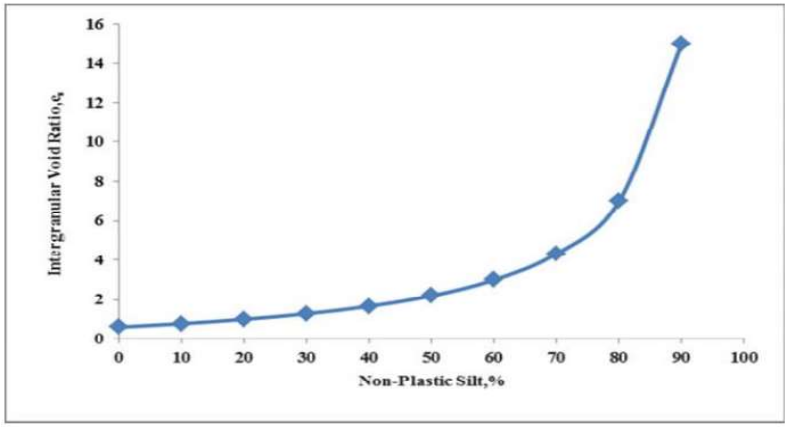

Fig. 43: Effect of non-plastic silt content on intergranular silt content. [Banupriya et al. (2015)]

Karim and Alam (2017) study the Effect of non-plastic silt content on undrained shear strength of sand–silt mixtures. The sand used in this study is collected from Padma River, Bangladesh and classified as poorly graded Sand (SP). Static undrained triaxial test were performed to determine undrained properties of silty sand. Silt (Non Plastic) is mixed with sand with different proportion was 10%, 20%, 30% and 60%. A test on pure silt was also conducted. The undrained monotonic triaxial tests were performed on sand–silt mixtures at 30%, 60% and 78% relative densities (initial relative density) and under the effective isotropic confining pressure of 100 kPa at strain rate 0.05% per minute till maximum axial strain 15% (ASTM-D4767-02).

A term “Limiting fines content” is discussed in this literature which is defined as a transition point below which the soil structure is generally a sand dominated one with silt contained in a sand-skeleton whereas beyond this point there are enough fines such that the sand grains loose contact with each other and the soil structure becomes predominantly a silt dominated one. The LFC is generally calculated using the following expression:

$$LFC = \frac{W_{fines}}{W_{sand} + W_{fines}} = \frac{G_f e_s}{G_f e_s + G_s(1 + e_f)}$$

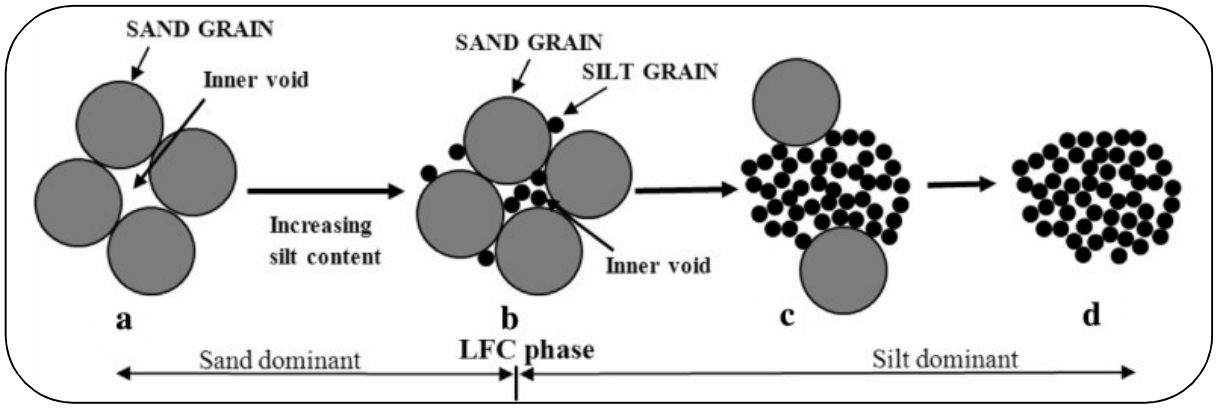

Fig. 44 : Visualization of limiting fines content

[Karim and Alam (2017)]

Results of different relative densities are discussed separately in the literature. After combining all experimental results together it can be concludes that:

- Limiting fines content (LFC) was found to be the very important parameter to understand the behaviour of sand–silt mixture. The behaviour of sand–silt mixture changes approximately at LFC.
- As the silt content increase monotonic peak shear strength decrease up to LFC and silt content more than LFC, monotonic peak shear strength remains constant with increasing silt content.
- It is seen that for same relative density, dry density increases slightly with increasing silt content up to LFC and again decreases with increasing silt content more than LFC.
- At constant global void ratio, the peak shear strength decreases with increase in silt content till LFC and for further increment of silt content the peak shear strength increases.
- Permeability is decreasing with increasing silt content up to LFC. After the LFC, dry density is decreasing with increasing silt content but permeability remains constant till pure silt.

Varghese et al. (2019) conducted study on undisturbed soil samples (UDS) from various depths from a site in the Western region of the IGP (Indo Gangetic Plain) to determine its cyclic and post-cyclic characteristics. The modulus degradation and damping behaviour of UDS samples are determined for low, intermediate and high strain levels. The soils used for experiments are SM, ML type soil. Low strain, intermediate strain, and large strain tests using the bender element, resonant column, and cyclic triaxial apparatus respectively were carried out in the test program. Beside this, the post cyclic behaviour was obtained using cyclic triaxial apparatus. The test samples for all the tests with 50mm diameter and 100mm length were prepared by carefully trimming the UDS samples of 70mm diameter using a wire cutter.

The maximum shear modulus of the soils was determined using the bender element apparatus. The shear wave velocity and the maximum shear modulus at different depths are presented in the table below:

Maximum shear modulus of soil at different depths.

Depth (m)	V_s (m/s) Present study	G_{max} (MPa) Present study	G_{max} (MPa) [52]	G_{max} (MPa) Seed & Idriss ([70]	G_{max} (MPa) Chattaraj & Sengupta [6]
6.5	186	62	71	62	71
10	204	81	99	68	98
22	232	102	124	97	120
32	292	171	149	132	142

The strain dependent shear moduli of the soil up to 0.05% strain were determined using resonant column tests. The resonant frequency is identified as the minimum frequency to attain the maximum amplitude (Amax), obtained from the frequency response curve.

The modulus degradation curves proposed for the Haryana region of the IGP, obtained from tests on UDS samples from are found to be in agreement with those proposed for similar soil conditions, by researchers in the past. However, the damping curves are found to exhibit a milder slope in comparison to standard curves.

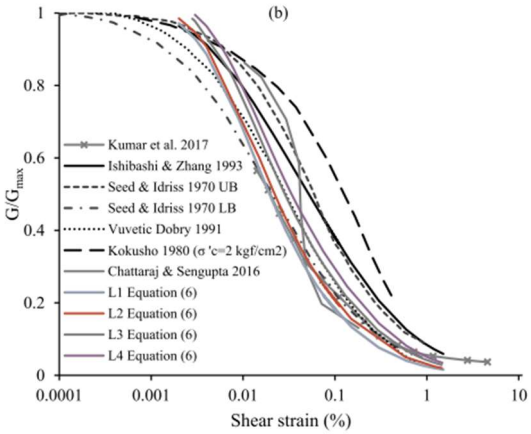

Fig.45:Strain dependent normalized shear modulus and (b) proposed modulus degradation curves, for layers L1, L2, L3, and L4. [Varghese et al. (2019)]

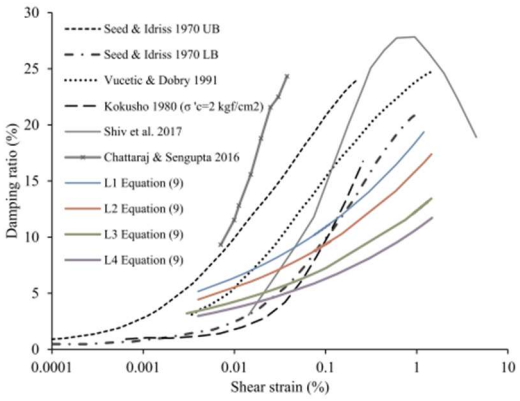

Fig.46:Proposed damping ratio curves for various soil layers from the present study [Varghese et al. (2019)]

Based on the experimental data, the modified expression for the modulus degradation curves that expresses G/G_{max} as the product of a decreasing function of shear strain, γ and a function of the mean effective confining pressure (σ'_c) is:

$$\frac{G}{G_{max}} = 0.5 * \left(1 + \tanh\left(\ln\left(\frac{8.2834 * 10^{-5}}{\gamma}\right)^{0.5971}\right)\right) * \left(\sigma'^{0.272*}_{c}\right) \left(1 - \tanh\left(\ln\left(\frac{6.4162 * 10^{-4}}{\gamma}\right)^{0.3915}\right)\right)$$

Kumar et al. (2020a) took specimens of sandy soil, prepared at two different relative densities (30% and 90%), were subjected to different effective confining stresses, and sheared monotonically as well as cyclically. The measurements from the on-sample transducers were further used to determine the modulus degradation curve for low-strain (less than 0.01%) to high-strain (greater than 1.0%). Maximum shear modulus estimated from the cyclic tests is found to have an agreeable match with the same obtained from the monotonic tests corresponding to very low strains, as well as with those obtained from standard correlations.

The small-strain shear modulus computed from the local strains, for both monotonic and cyclic tests, is found to have reasonable agreement with those obtained from standard empirical correlations. The localized strain measurements also help to identify the dynamic shear modulus of the soil over a wide range of strain. Beyond cyclic shear strain amplitude of 0.1%, the modulus reduction curve obtained from the on-sample LVT measurement agrees excellently with the same estimated from external LVDT measurements. Local measurement of axial and radial strains from on-sample LVDTs resulted in the identification of the strain-dependent Poisson's ratio of the specimen during shearing. Thus, on-sample LVDTs are found to be efficient to determine the dynamic behaviour of soil over a wide strain range, encompassing both low-strain (approx. 3 $x10^{-3}$%) and high-strain (greater than 1.0%) ranges, and that too without the usage of any other sophisticated tests such as the bender element and resonant column tests. It is shown that the on-sample LVDTs can be effectively used for the evaluation of the strain-dependent dynamic shear modulus even for the specimens having very low relative density and subjected to low confining pressures.

Kumar et al. (2020b) examined the monotonic and dynamic properties of riverbed sand and hill slope soil of North east India. Three types of soil are taken for the experiment those are cohesionless soil (i.e. Brahmaputra riverbed sand, or BS), cohesive soil (Red soil, or RS) and silty-sand soil (or SS), collected from Guwahati region, Assam (India).All the tests were conducted on the remoulded cylindrical soil specimens of dimensions 70 mm diameter and 140 mm height. Cohesionless BS and Cohesive RS soil are tested under three different confining pressure (50 kPa,100 kPa,150 kPa) to find out stress-strain response of soil under monotonic condition. On the other hand, silty-sand soil (or SS) is tested with 100 kPa and 200 kPa.

After extensive experiment it is observed that under monotonic loading, the shear stiffness of the cohesionless BS soil is predominantly influenced by initial relative density of the prepared sample than the applied confining pressure or displacement loading rate. For the cohesive RS soil subjected to monotonic loading, although the confining pressure exhibits significant influence on the stress–strain behaviour, the secant modulus remains nearly unaffected by the change in the confining pressure. On the other hand, the stress–strain response of silty-sand SS soil is significantly affected by the change in the confining pressure. Under monotonic loading, both RS and SS soils are significantly influenced by the

degree of saturation of the prepared sample. From the dynamic tests, it is concluded that the strain-dependent shear modulus (G) increases with the increasing $\sigma_c$while the modulus reduction ratio, G/G_{max}, is negligibly affected. The damping ratio, D, is found to be marginally affected by the changes in σ_c. From the present study, it is concluded that, irrespective of the soil type and applied effective confining stress, the damping ratio decreases beyond 1% shear strain, which a major difference from the standard propositions.

Chakrabortty et al. (2020a) conducted a series of strain-controlled cyclic triaxial tests on isotropically consolidated soil specimens. The fine sands used in this study were collected from the Ganga and Sone river bed.The samples were prepared with 100% non-plastic silt, 100% sand and different percentage (5%, 10%, 20%, and 30%) of non-plastic silt mixed with fine sand.Researchers suggested that the specimen prepared using a dry deposition technique replicates the natural deposition of sand. So, the dry air pluviation method has been adopted in this study as it maintains uniformity in soil specimen. The soil samples were prepared in a split mould of 38 mm diameter and 76 mm height at low relative density (D_r)between 10 and 25% . Total 18 no of cyclic triaxial test were conducted.

After conducting these tests , they found that higher rate of excess pore water pressure generation has always been observed for the soil specimen prepared with 100% non-plastic silt at all strain levels. The rate of excess pore water pressure generation was initially found to decrease till 20% and 10% non-plastic silt content in Sone and Ganga sand, respectively. Among Sone and Ganga sand, the liquefaction susceptibility of Ganga sand has been found higher than Sone sand at the same relative density, confining pressure, strain level and fines content. Hence, it can be stated that with the increase in $D_{50\ sand}$ /$D_{50\ silt}$ ratio, the liquefaction susceptibility of sand decreases. They also found that in case of Sone river sand at various axial strain levels (i.e., 0.13%, 0.66% and 1.31%), it was found that the effect of non-plastic silt intrusion in the sand could be observed at the lower strain level. The liquefaction resistance of sand decreases with the increase in non-plastic silt proportion at axial strain level of 0.13%. However, at higher axial strain amplitudes (0.66% and 1.31%) the number of cycles required for liquefaction was observed almost the same for the soil specimen with 0%, 20% and 100% non-plastic fines.

Chakrabortty et al. (2020b) conducted a series of undrained cyclic triaxial tests on the partially saturated fine and medium-grained sand samples. The samples were prepared either at a very loose compacted condition (RD≤20%) or at dense relative density (RD≥60%), to quantify the effect of S_r on the dynamic behaviour of cohesionless soil. The Skempton's coefficient B for these triaxial tests varies from 0.11 to 0.87, which represents the variation in the S_r ranging from 86 to 99%. From the detail discussion on these test results, various conclusions were drawn in this study.

Shear modulus at large strain for both fine and medium grained soil decreases with the increase in the degree of saturation. They mentioned the possible reason as the presence of occluded air bubbles in the pore water of partially saturated fine and medium-grained sand.

The fine grained sand was found to be more affected due to the change in the S_r as compared to medium-grained sand because of the presence of more voids in the soil structure. However, both sands show dilative behaviour (‘‘no flow’’ condition) under cyclic load at a lower S_r instead of very low relative density. At a higher S_r (above the threshold limit of Skempton’s B-value) both sands show a limited liquefaction behaviour (‘‘flow’’ condition) under cyclic loading.
The damping ratio was also affected due to the variation in the degree of saturation. A decreasing trend in the damping ratio was observed in this study for both medium and fine-grained sand with the increase in Skempton’s coefficient B. This phenomenon was observed due to the contribution of the inter-particle water lubrication mechanism at different saturation condition.

Marzunietet al.(2021) conducted study on sand and non-plastic silt were used in this study to determine the simultaneous effect of cyclic stress ratio(CSR) and non-plastic fines content at a constant pressure on the liquefaction of silty-sand through cyclic triaxial testing.Clean sand to 70% sand with 30% silt, 40% sand with 60% silt, and pure silt were tested under different CSR values i.e. CSR=0.1,0.15 and 0.2. The results showed that an increase in the silt content up to 30% decreased the liquefaction resistance. At a 40% sand and 60% silt, the resistance increased. In the samples with up to 70% sand and 30% silt, the settlement of fine particles of silt filled the spaces between the coarser particles of sand and reduced the ability of the soil to drain during an earthquake or cyclic loading vibrations. The result was an increase in the liquefaction potential under these conditions. An increase in the silt content of more than 30% caused the soil to behave as fine-grained soil and the liquefaction potential decreased.

The effect of CSR on the liquefaction behaviour of all soil samples was evident in this study. The four samples containing different amounts of silt showed different strain behaviour at different CSR values. As the CSR changed, the order of pore water pressure generation of the different samples varied. Furthermore, axial strain in all types of soil up to $r_u = 1$ at CSR = 0.15 was more uniform than at CSR = 0.2.

They observed that at CSR = 0.2 the curves forr_u versus the number of cycles for the four types of soil are approximately the same. However, at CSR = 0.15, the curves deviate from one another. The most rapid increase in pore water pressure was for S7M3, and the behaviour of the other soil types with a change in CSR differed.

Sharika and Kumari (2023) investigate the performance of Gangetic sand obtained from the Indo-Gangeticriver basin by examining its static and dynamic behaviour using triaxial tests. Static as well as cyclic trials were extended for similar three confining pressures and two different densities. The static behaviour of the Gangetic Sand was examined on the basis of stress–strain, effective stress path, and pore pressure generation. In addition to the above, the

evolution of cyclic stress ratio and dynamic properties including degradation of shear modulus and damping coefficient were analyzed while assessing the cyclic behaviour.

Results obtained from the experiments shows that loose samples under lower confining stress (50 and 100 kPa) were found to be vulnerable while dense samples due to their dilation were observed to be safe against liquefaction. For the dynamic trials also, a nearly uniform behaviour was observed for the loose and dense samples under lower confining stresses, while a greater strength reduction is observed for the higher pressure. So, the loose Gangetic sand is vulnerable to liquefaction under lower confining stresses. Under dynamic loading, irrespective of density, samples with lower confining stress exhibit liquefaction within 10–15 cycles, while 200kPa samples show only strength reduction even after 50 loading cycles.

3. Experimental Program

3.1 Material used

Fine sand sample used in this study were collected from the Tollygaunge area of Kolkata city. Collected soil sample were oven dried and then sieved through the respective sieve sizes. The soil is classified as "Uniformly graded sand" with fine content of 6%. The grain size distribution curve is shown in the figure 47.

The maximum and minimum void ratio indexes are found using vibration table method. e_{max} and e_{min} are obtained as 1.17 and 0.68 respectively. Specific gravity of the soil is found to be 2.69. The other parameters are shown in the table 1.

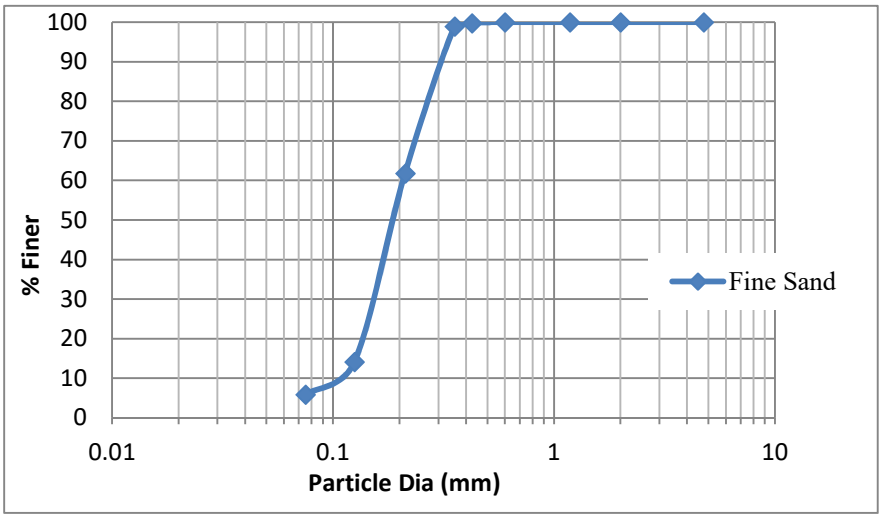

Fig. 47: Grain size distribution of sample used in this study

Table 1: Physical properties of the soil used in this study

Physical Properties	Value
Mean Grain Size D_{50}	0.18
Uniformity Coefficient (C_u)	1.75
Coefficient of Curvature (C_c)	1.02
Specific Gravity (G_s)	2.69
Maximum Void ratio (e_{max})	1.30
Minimum Void ratio (e_{min})	0.68
Maximum Dry density (g/cc)	1.17
Minimum Dry density (g/cc)	1.60
D_{60}	0.21
D_{30}	0.16
D_{10}	0.12
Classification	SP

3.2 Preparation of Soil Sample

Soil specimens used in this study were of 75 mm in diameter and 150 mm in height. There are various methods of preparing soil specimen such as dry funnel deposition method, water sedimentation method, moist tamping method, slurry deposition method etc. Among them moist tamping method was adopted for this study. In this method we can easily make the lower relative density as well as higher relative density. Firstly, desired amount of dry sample is taken and the total sample is divided into 6 parts. Each part is kept in one container and 10% of water (percent of dry weight of soil) is added to each container. Then the each soil sample is thoroughly mixed with the help of spatula. Then the split mould is taken and the rubber membrane is attached inside the mould. A small amount of vacuum pressure is given to ensure close contact between the rubber membrane and the inner side of split mould. After that, one porous stone and filter paper is placed at bottom of the mould. Then moist soil sample from each container is poured into the split mould and compacted using a light weight hammer. After pacing the last layer of soil, another porous stone and one filter paper is placed on the top of the soil sample. The number of blows per each layer and corresponding height of fall is determined by trial to achieve target relative density. In order to obtain a uniform density throughout the specimen, the compaction method of specimen preparation suggested by Ladd [1978] was followed.

When the sample preparation is completed, the vacuum pressured is detached from the split mould and split mould is carefully taken to the sample base. After that, the extra portion of the membrane was unfolded at the bottom and top of the sample. The height of the membrane was maintained two times as the sample so that it can cover the top sample cap and sample base grooves. Then split mould is detached from the sample very carefully so that no disturbance is happen. One O-ring is placed at bottom groves of the sample base with the help of a hollow cylinder which diameter is slightly greater than sample diameter. Then the sample cap attached with submersible load cell is kept on the sample top and extra portion the membrane is unfolded over the sample cap and O-ring is placed on the groove for proper sealing. Once the cell chamber was assembled, the de-aired water filled in it through the cell pressure line.

Fig.48: Soil sample after preparation gripped by Split mould and rubber membrane

3.3 Saturation of Soil Sample

Saturation of soil specimen is necessary to provide reliable measurement of pore water pressure and volume change. In an undrained triaxial test, the condition of no volume change may be simulated if the specimen is completely saturated. In this study, saturation of the sample is done by flushing of gaseous CO_2 followed by passing de-aired water throughout the sample. Before CO_2 flushing, confining pressure of about 40 kPa is given so that disturbance in the sample becomes less. After the giving the confining pressure, gaseous CO_2 is introduced through the bottom drainage line, thereby pushing the lighter air in the specimen out through the top drainage line. The CO_2 is allowed to seep up through the specimen for 15-30 min, ensuring complete replacement of air, which is lighter than CO_2. In this stage, the pressure of the CO_2 is constantly monitored so that it does not greater than the applied confining pressure. Next stage is water flushing. De-aired water from another water chamber is introduced through the bottom drainage line and also allowed to seep slowly up through the specimen, thereby pushing most of the CO_2 out through top drainage line. Any CO_2 left in the specimen will dissolve in the intruding water, which in turn will fill the voids in the specimen. This process of water continues until a uniform flow of water is achieved through the top drainage line. This process takes 5-15 min to complete.

Fig.49 : Process of Saturation of sample by flushing of gaseous CO_2 through the soil sample

3.4 B Value Check

For laboratory testing of soils, standards and code specify that a soil sample can be considered to be fully saturated if Skempton's pore pressure coefficient B is over 0.95. Pore pressure parameter B-value is the size of the pore pressure response during an undrained loading increment prior to consolidation.

Fig.50: After mounting the sample on triaxial base

Once the water flushing is completed, confining pressure line, back pressure line and pore pressure line are connected to the triaxial cell. Then the CP (Confining pressure) and BP (Back pressure) are increased simultaneously keeping the difference between them as low as 20kPa. In this stage, 'B' value is checked by increasing the CP and measuring the PP (Pore Pressure) increased due to increase in CP keeping the BP line closed. If the value of 'B' is greater than 90%, then the saturation is achieved. Otherwise, the further increase the CP and BP and wait for some time and again check the 'B' value. This process continues until satisfactory saturation is achieved.

3.5 Consolidation of soil sample

At this phase of consolidation, the CP is increased and BP is adjusted so that the effective confining stress becomes 100 kPa. All the samples tested in this study were isotropically consolidated to a desired effective confining pressure of 100 kPa. The sample was kept in this position until volume change becomes constant. The duration of the process of consolidation takes 15-30 min to complete.

Fig.51 : After completion of consolidation Phase before shearing of the sample

3.6 Shearing of the sample

This is the final stage of cyclic triaxial test. Once the consolidation phase ended, sample becomes ready for shearing. At this stage dynamic actuator is turned on and checked if everything is ok. After that the triaxial cell is brought under the dynamic loading frame and connects the dynamic actuator with the triaxial cell set-up. Then the amplitude, frequency, type of loading, number of cycle of the cyclic loading is set in the computer system. Finally, the test is started after closing the BP line.

Fig.52 : During shearing of the sample

Fig.53: Pneumatic control panel for the application of confining pressure, back pressure and vacuum.

Fig.54: Monitor, CPU, Triaxial Cell and Loading frame

3.7 Study Combinations

Table 2: Combinations of study for the strain controlled cyclic triaxial tests

Relative Density (%)	Peak Axial Strain (%)	Frequency (Hz)
35	0.33, 0.67	1
60	0.33, 0.67, 1.0	1
60	0.67	0.1, 0.5
75	0.33, 0.67	1
90	0.33, 0.67	1

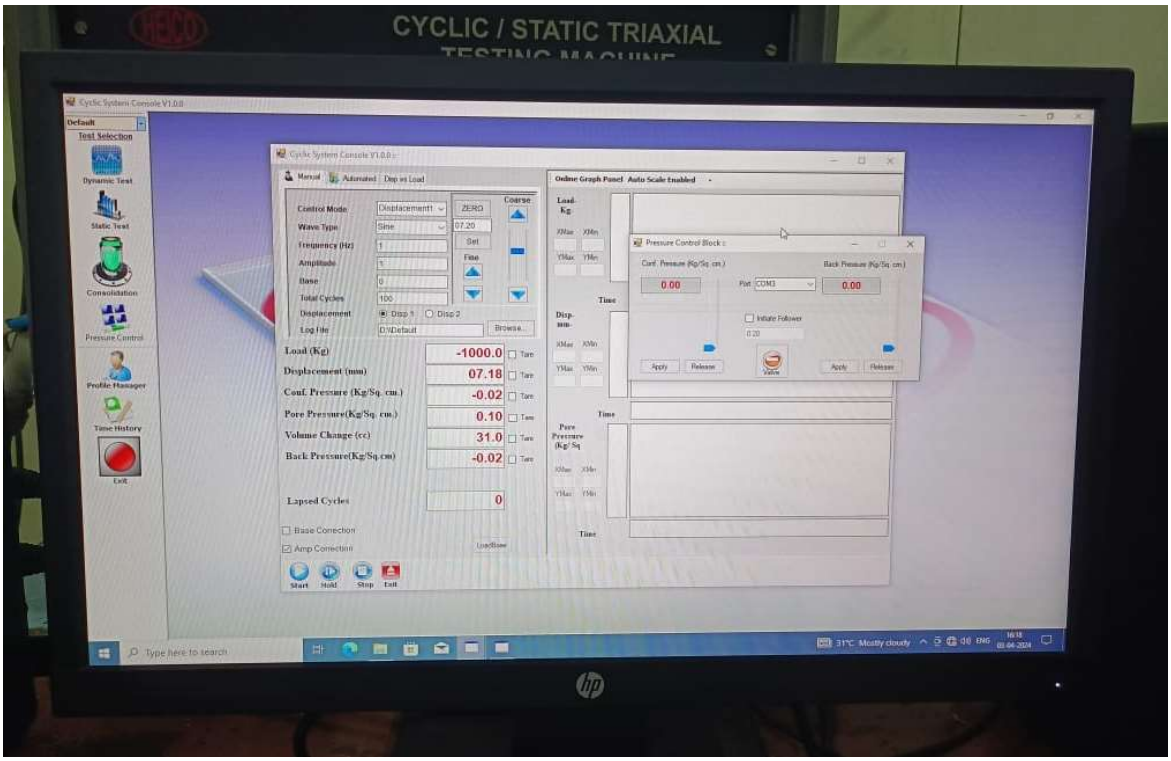

Fig.55: Cyclic system console V1.0.0 developed by Heico

4. Results and Discussions

The undrained cyclic triaxial tests were performed on sandy soil sample at different relative density of 35%, 60%, 75% and 90%. All the samples were isotropically consolidated at effective confinement of 100 kPa. Then, the samples were sheared under constant effective confining pressure of 100 kPa and three peak axial strain of 0.33%, 0.67% and 1.0%. Also, frequency of cyclic loading was varied for 60% relative density to determine its effect on dynamic soil properties. Three different frequencies of 0.1 Hz, 0.5 Hz and 1 Hz were used in the case of 60% relative density. Total 11 numbers of tests were performed on the soil sample which is given in the table 2. Strain controlled approach was adopted for testing. The shape of the loading was selected as sine curve.

No of cycles for Liquefaction and dynamic soil properties such as shear modulus and damping ratio were determined for each soil specimen after getting data from cyclic triaxial test.

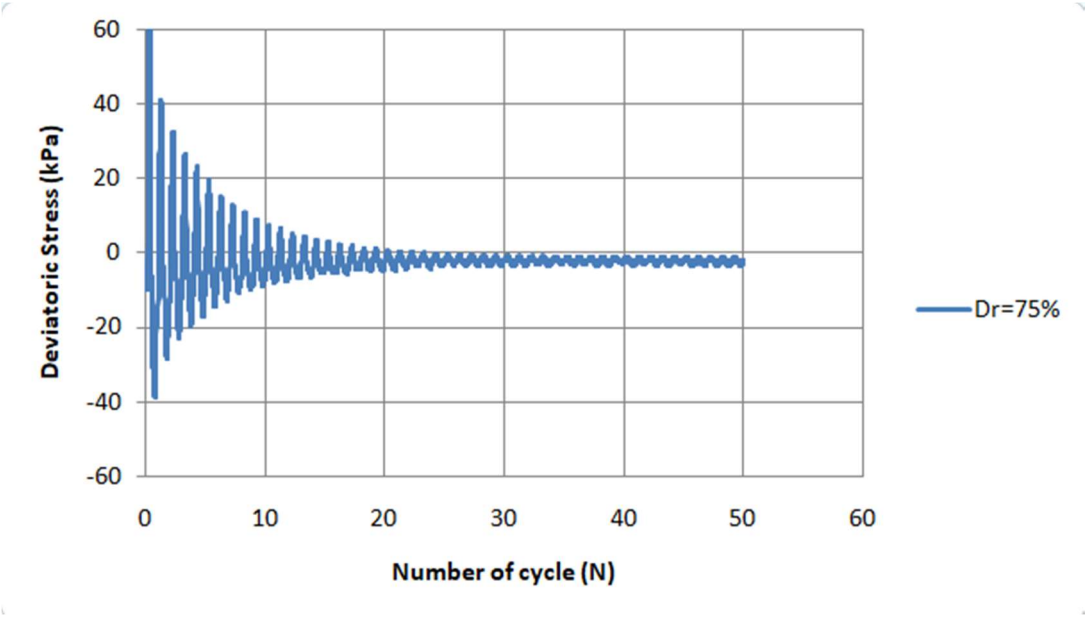

Fig.56: Plot of Deviatoric stress Vs Number of cycle at Dr=75%, γ=1.0%

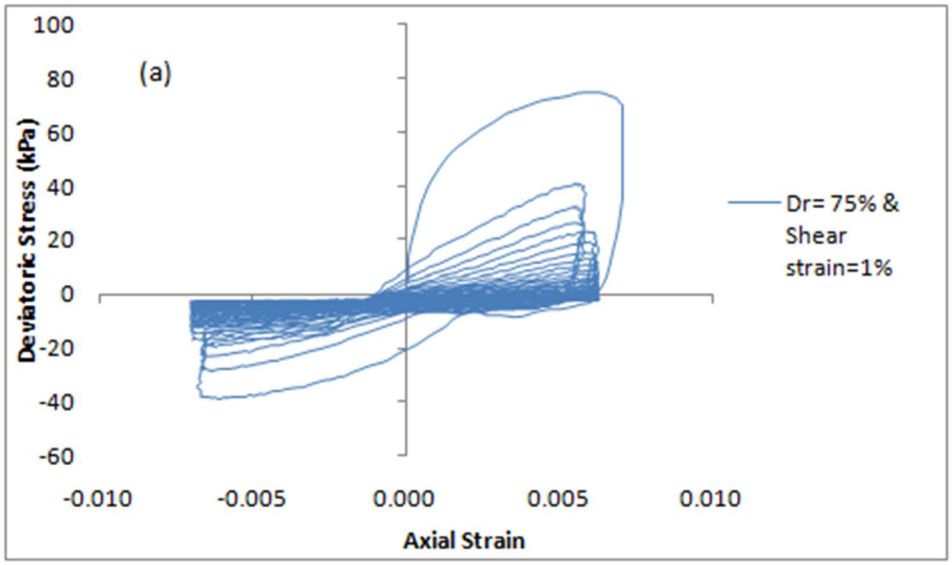

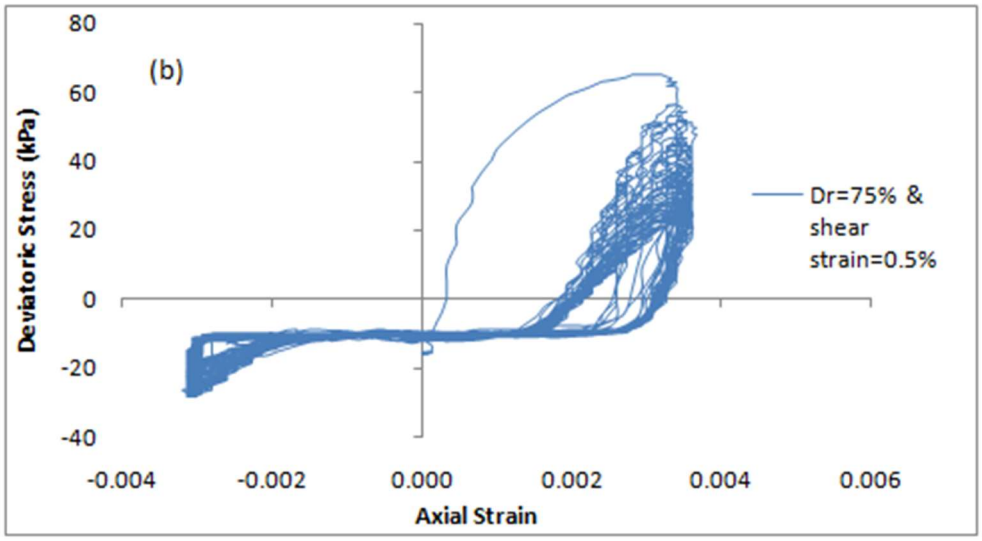

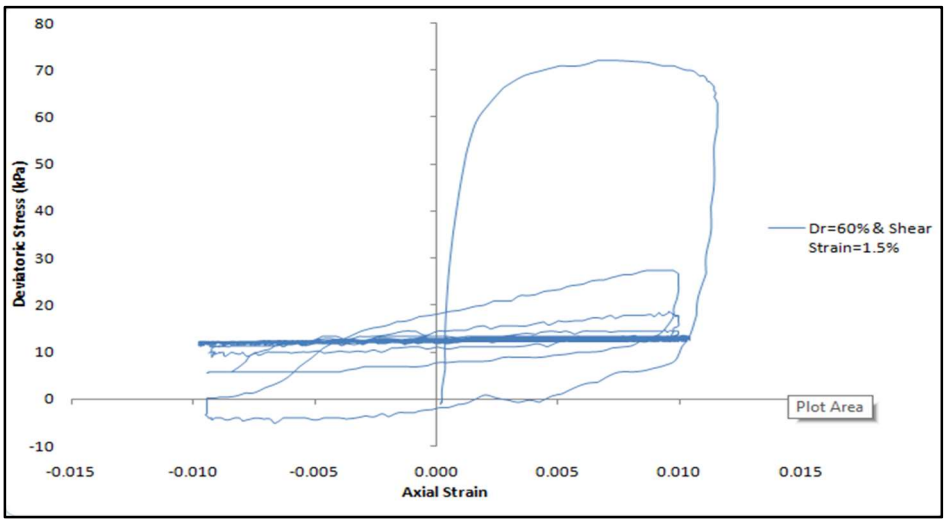

Fig.57: Plot of Deviatoric stress (kPa) vs Axial strain (a) Dr=75% & γ=1% (b) Dr=75% & γ=0.5% (c) Dr=60% & γ=1.5%

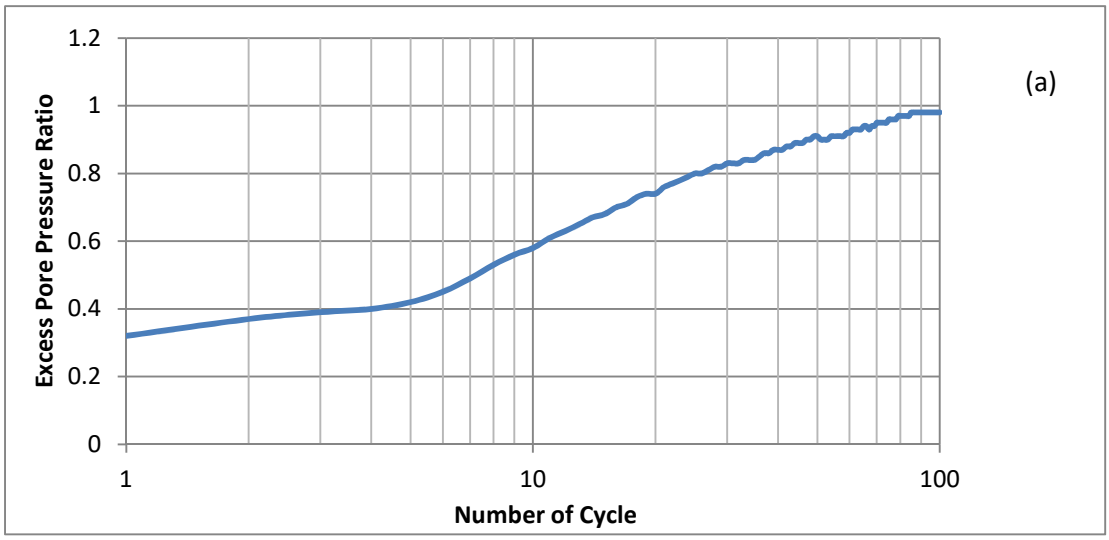

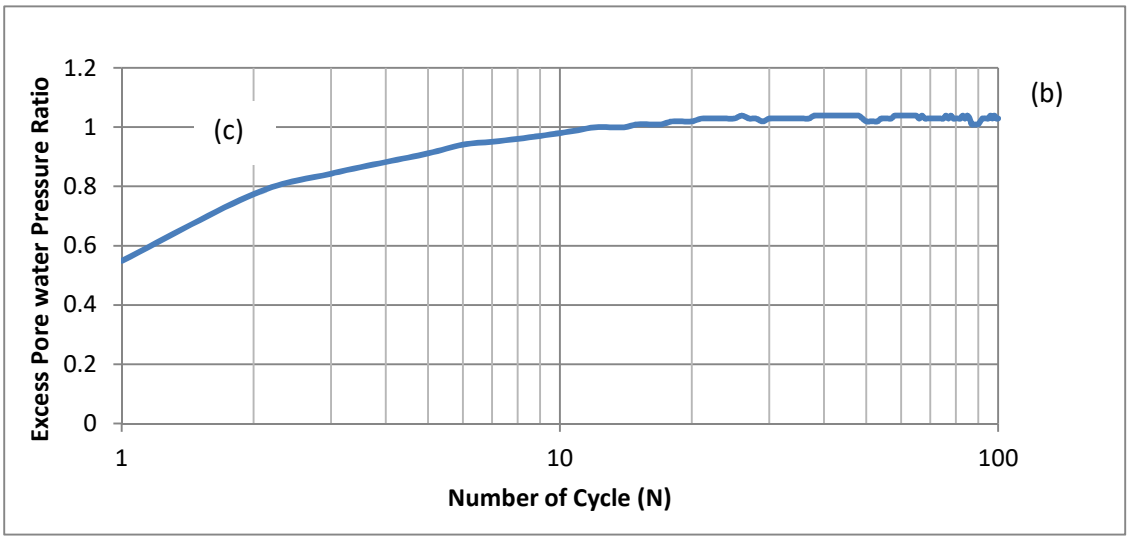

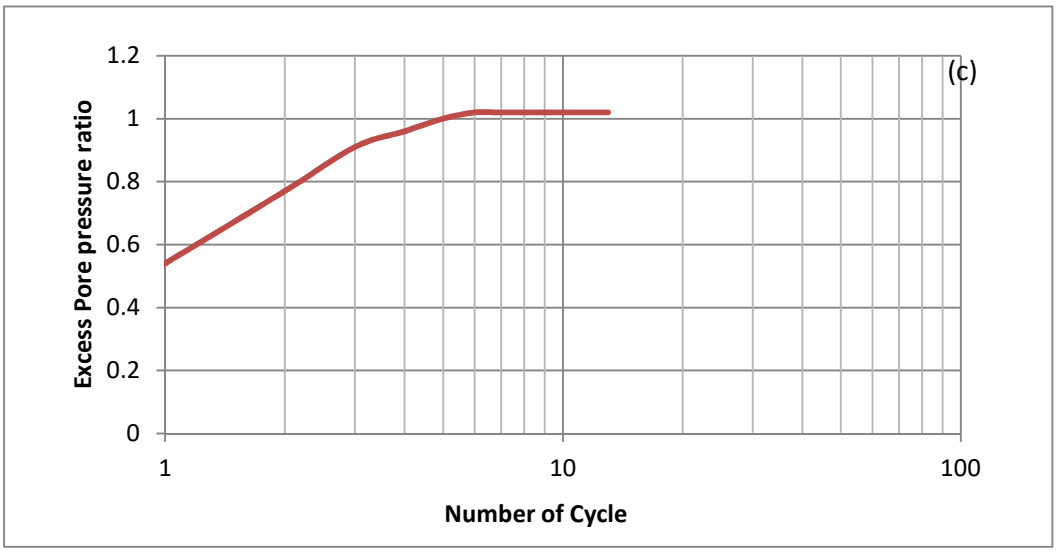

Fig.58: Plot of excess pore pressure ratio vs number of cycle (a) Dr=60% & γ=0.5% (b) Dr=75% & γ=1% (c) Dr=60% & γ=1.5%

4.1 Liquefaction Results

Liquefaction is a phenomenon in which the strength/stiffness of loose, saturated, cohesionless soil is reduced due to increase in pore water pressure caused by any dynamic loading such as earthquake or machine vibration. Earthquakes are the most common cause, as the cyclic loading from seismic waves increases pore water pressure within the soil. Liquefaction happens when the excess pore water pressure becomes equal to the effective confining pressure of the specimen. Liquefaction is often represented using pore water pressure ratio (r_u), which is the ratio of excess pore pressures (ΔU) generated in the soil column to the mean effective confining pressure (σ'). Figure 59 represents the variation of the excess pore water pressure (PWP) ratio and cycle of loading (N) at 100 kPa confining pressure for 60% relative density (D_r).

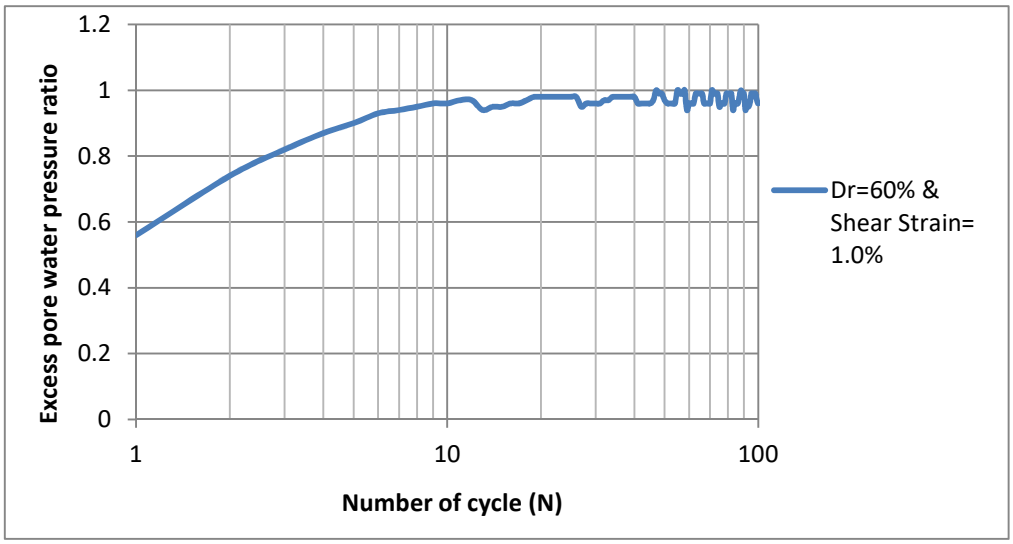

Fig.59: Typical variation of excess pore water pressure ratio with number of cycle for 60% relative density and shear strain of 1.0%

4.1.1 Effect of shear strain (ϒ) on Liquefaction resistance

Figure 60 depicts that the variation of PWP ratio with number of cycle (N) at different shear strain (γ) and a constant relative density (D_r) of 60%. It can be observed that higher the shear strain (γ), higher is the liquefaction potential. In other words, for the same value of number of cycle (N), tendency to liquefy the specimen increases with increasing the shear strain (γ) at a particular relative density (D_r). Figure 9 also depicts that the soil specimen attains $r_u \geq 0.90$ in the 2nd cycle at γ=1.5%, thus revealing the onset of liquefaction at 2nd cycle (N=2). Whereas the more N are required to initiate liquefaction for soil specimen subjected to γ=0.33% and Γ=0.67%. Rate of increase of PWP for shear strain of 0.5% is very slow as compared to shear strain of 1.5% and 1%. Figure 61 shows the variation of number of cycle for liquefaction (N) with shear strain for the samples of 60% relative density. It is clearly observed from the

figure 61 that as the shear strain increases the number of cycle for liquefaction (N_L) decreases rapidly. It is also evident that both curve corresponding to r_u=1.0 and r_u=0.9 decreases in the same pattern.

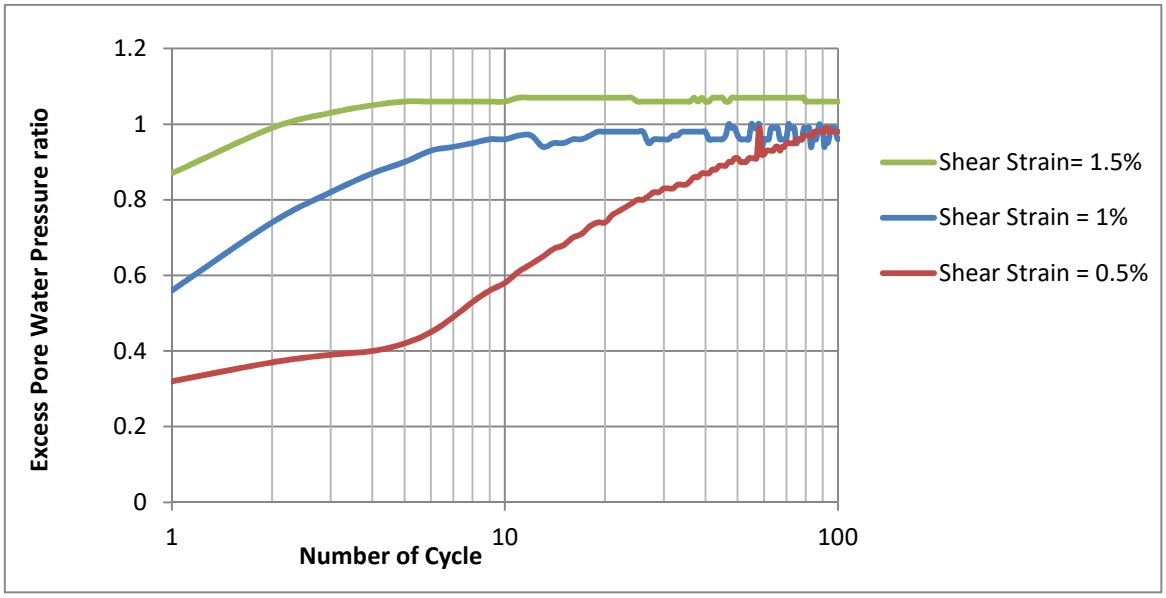

Fig.60: Plot of variation of excess pore water pressure ratio with Number of cycle (N) at different shear strain(ϒ)

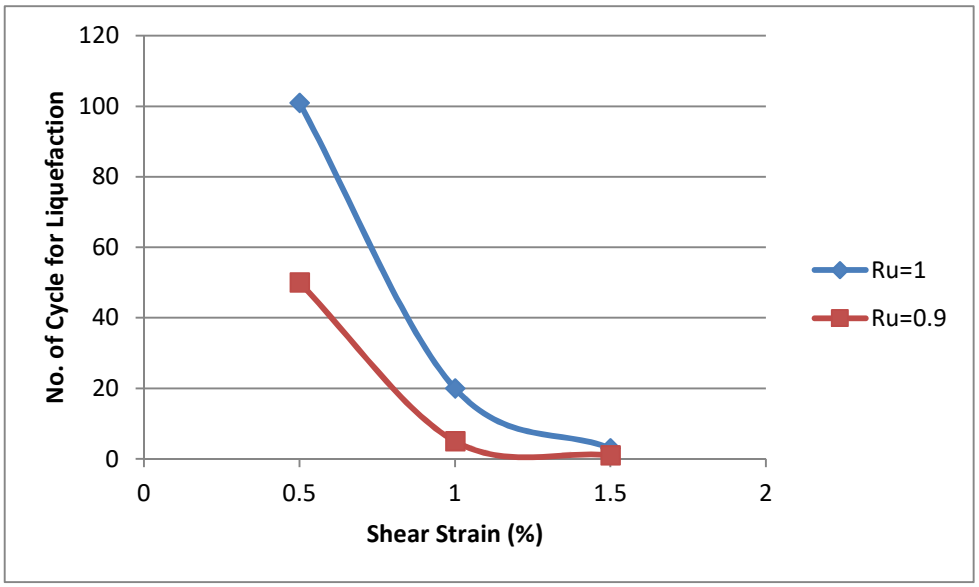

Fig.61: Plot of Number of cycle for liquefaction Vs shear strain (ϒ) at a constant relative density of 60%.

4.1.2 Effect of relative density (D_r) on Liquefaction resistance

Figure 62 illustrates the variation of r_u with number of cycle (N) at different relative density (D_r) i.e. 35%, 60%, 75% and 90% and at a constant effective confining pressure (σ_3') of 100 kPa. It is reflected from the study that the excess pore water pressure ratio (r_u) decreases with the increase of relative density (D_r) means at higher D_r, higher number of cycles (N) are required to liquefy the soil specimen for a constant shear strain (ϒ) and constant effective confining pressure (σ_3').So, the liquefaction resistance increases with increase in relative density. It can be observed from the study that the number of cycle required for liquefaction (N_L) for the sample of 90% relative density is about 5-6 times higher than the number of cycle required for liquefaction (N_L) for the sample of 35% relative density. It can be also depicted from the figure 60 and figure 62 that the excess pore water pressure for the very first cycle is significantly affected by the shear strain whereas, the same is marginally affected by the relative density.

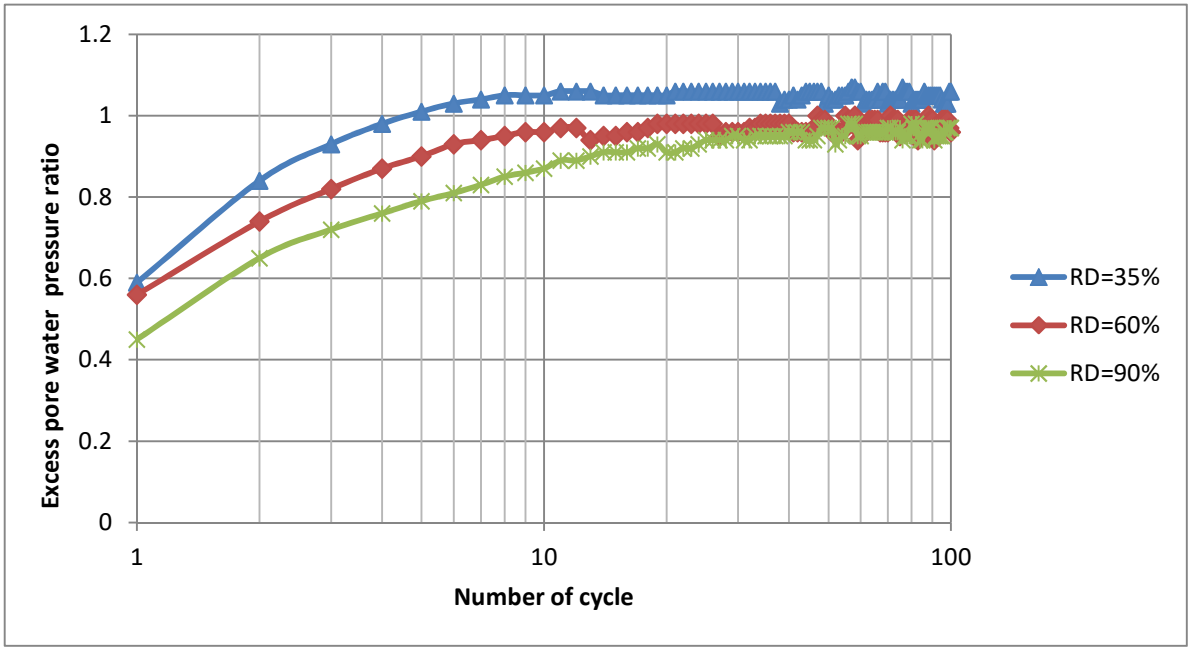

Fig.62: Plot of excess pore water pressure ratio with number of cycle at different relative density of 35%, 60% and 90%

Figure 63 illustrates the variation number of cycle for liquefaction (N_L) with relative density at a shear strain (ϒ) of 1%. Cycle required for attaining the excess pore water pressure ratio r_u=0.9 and r_u=1.0 is determined for different relative density and plotted in the following figures. It is observed the graph that at a constant confining pressure of 100 kPa, with increases in the relative density of the specimen the number of cycles for the liquefaction (N_L) increases profoundly. This behaviour can be explained in the way such as during cyclic loading, denser sands tend to contract less compared to loose sands. This results in lower excess pore water pressure build-up, thereby reducing the risk of liquefaction. Whereas, loose

sands tend to contract more during cyclic loading, leading to higher excess pore water pressure, which increases the chance of liquefaction

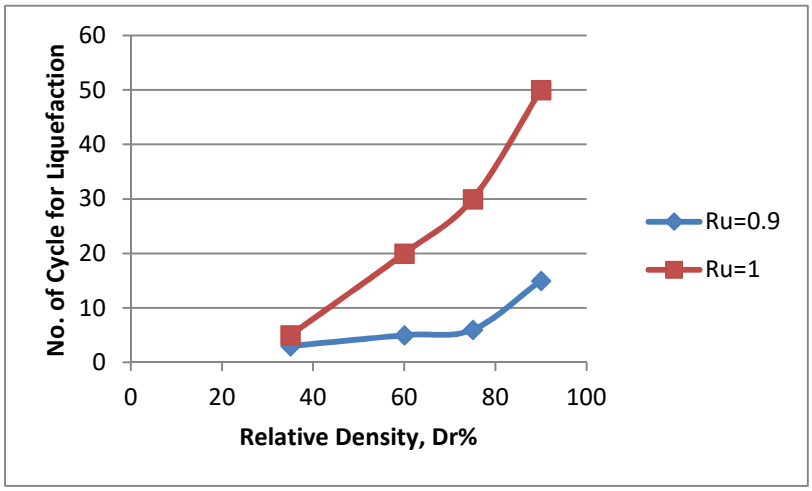

Fig.63: Plot of number of cycle for liquefaction (N_L) Vs Relative density (D_r) at shear strain of 1.0%

4.1.3 Effect of frequency on liquefaction resistance

The tests have also been conducted to obtain the effect of frequency of loading. The results depict that as the frequency increases, the number of cycles to reach liquefaction increases at same shear strain amplitude. At loading frequency of 0.1, 0.5 and 1 Hz, the failure cycles are observed to be 6, 12 and 20, respectively when the specimens are tested at 60% relative density and 1% shear strain. So, the study distinctly points out that the severity of loading increases at lower frequencies.

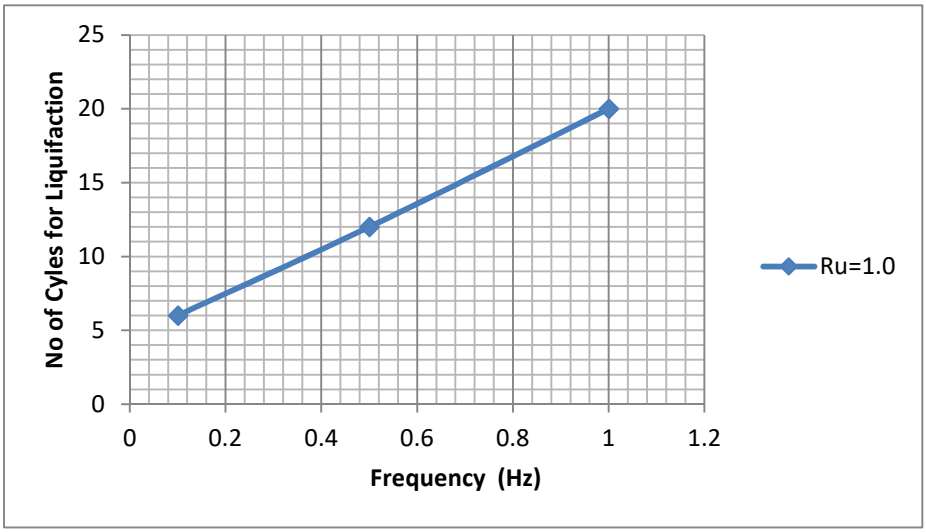

Fig.64: Plot of number of cycles for liquefaction vs frequency at Dr=60% and γ=1%

4.2 Evaluation of Dynamic soil properties

Dynamic soil properties i.e. shear modulus and damping ratio is to be evaluated to predict dynamic behaviour of soil under any dynamic loading. They are used to determine the safety of any structure or foundation lay on any seismic prone areas. Out of all loading cycles applied during the experimental study, dynamic soil properties i.e. shear modulus and damping ratio can be evaluated by considering any one particular hysteresis loop that is obtained from a particular loading cycle. Literature indicate the use of different loading cycle to compute the dynamic soil properties e.g. 1st cycle [Govindaru L 2005, Lanzo et al 1997, Vucetic M et al 1998, Rollins K M et al 1998, chung et al 1984 and Keyszig E 2010], 3rd cycle [Okur and Ansal 2007] and 10th cycle [Kokusho T 1980]. Matasovic and Vucetic 1993 have used separately the first cycle to compute shear modulus and 2nd cycle to compute damping ratio. The selection of the hysteresis loop was based on the assumption that up to nth cycle, the hysteresis loops remained symmetrical. In this study, shear modulus was estimated using 1st loading cycle and damping ratio was estimated using second loading cycle.

4.2.1 Conventional method for evaluation of dynamic soil properties

Figure 65 present a typical Symmetrical Hysteresis Loop (SHL), which portrays the suggested conventional method of calculation of dynamic soil properties. In this method, the dynamic shear modulus (G) is evaluated from the elastic Young's modulus (E_{sec}) which is obtained by the slope of the line joining the points of peak compressive and tensile stress-strain points. The procedure of evaluating the dynamic shear modulus is described as follows:

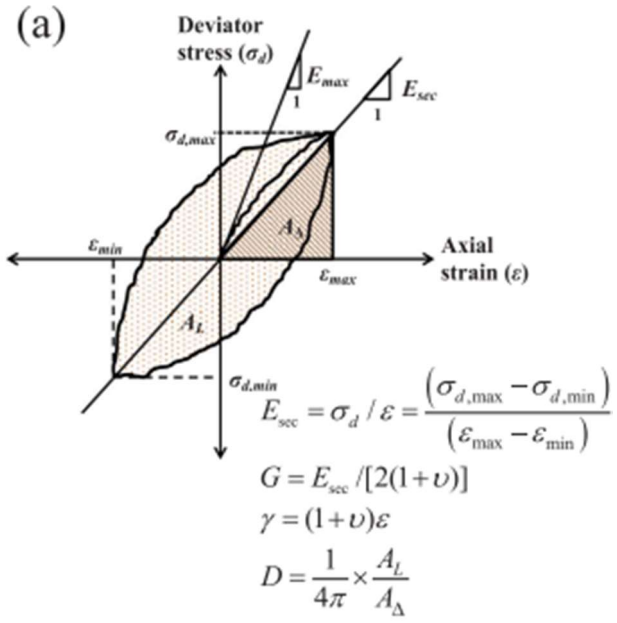

Fig.65: A typical hysteresis loop for evaluation of shear modulus and damping ratio. [Kumar et al 2017]

4.2.2 Modified method for evaluation of dynamic soil properties

Figure 67 presents the hysteresis loops for initial two cycles, from the strain-controlled cyclic triaxial test at peak shear strain of 1.0%. It was evident from the figure that the hysteresis loop obtained from the study is asymmetric in nature. In their literature Kumar et al 2017 suggested that in case of Asymmetric Hysteresis Loop (ASHL) as shown in figure 67, the conventional method will not yield appropriate value as it does not account the actual behaviour of soil. To take into the effect of actual strain energy and moduli value in compression and tension, true representation of asymmetric nature of hysteresis loop should be considered. Hence Kumar et al 2017 proposed a modified approach for evaluating the dynamic soil properties considering the asymmetric nature of hysteresis loop. The procedure for the modified method is as follows:

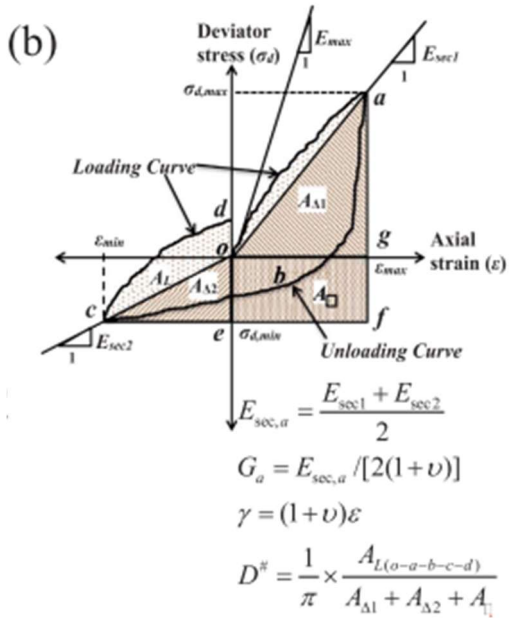

Fig.66: A typical asymmetric hysteresis loop for evaluation of shear modulus and damping ratio using modified method. [Kumar et al 2017]

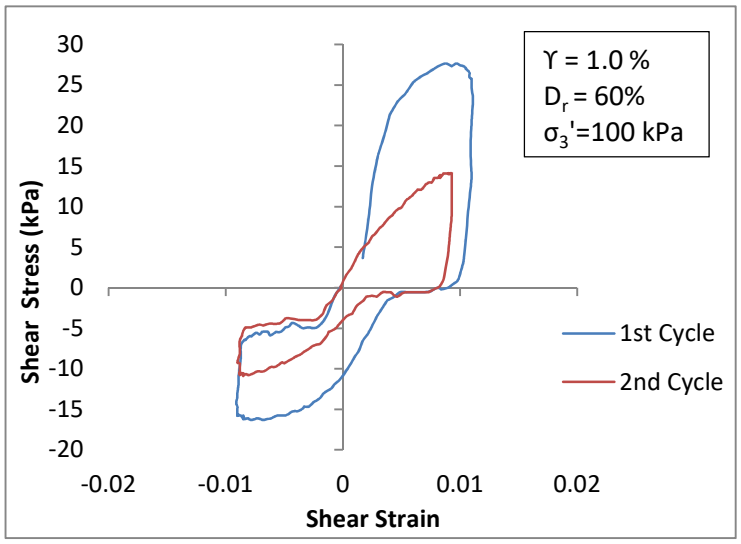

Fig.67: Typical shear stress-strain plot for initial two cycles at D_r= 60%, σ_3'=100 kPa and Υ= 1.0%

4.2.3 Evaluation of dynamic shear modulus (G)

Dynamic shear modulus (G) is first estimated using conventional method by considering the hysteresis loop to be symmetrical, where peak compressive and tensile stress-strain point are considered as same. Figure 68 represent the plot of deviatoric stress (σ_d) Vs axial stress(ε) for the peak shear strain of 1.0% at a relative density of 60%. The figure corresponded to the

very first cycle of loading. In the figure, if we join the origin with the peak axial stress point then the slope of the line gives the elastic Young's modulus (E_{sec}). Now using the formula the dynamic shear modulus can be obtained as follows.

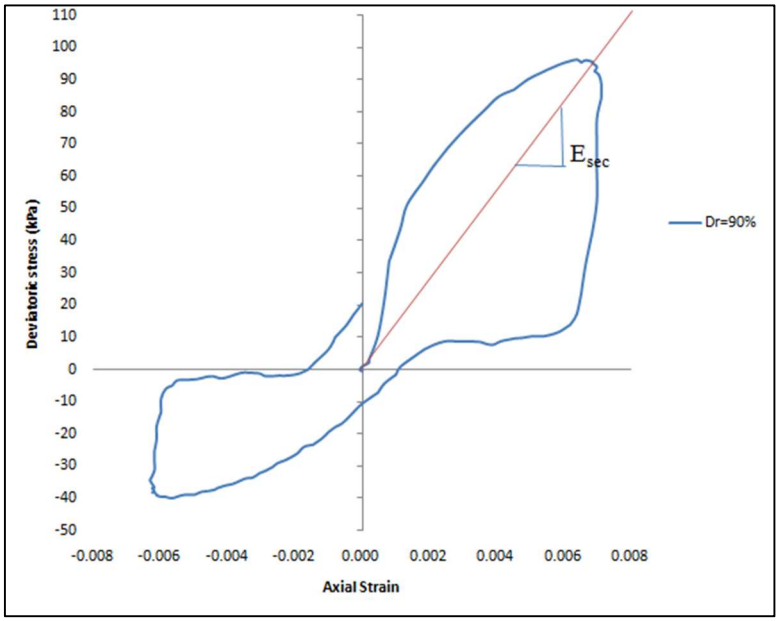

Fig.68: Plot of deviatoric stress Vs axial strain for Dr=90%, ϒ= 1.0% and f =1 Hz

- $E_{sec} = \frac{56-0}{0.004-0} = 14$ GPa
- $G_{sec} = \frac{Esec}{2(1+\nu)} = \frac{14}{2(1+0.5)} = 4.67$ GPa

As the hysteresis loop was asymmetric using modified method the shear modulus can be obtained using both compression and tension side of the loop. First join the both peak stress point. Then slope of the both line are calculated and average value of these slope give the elastic Young's modulus ($E_{sec,a}$). Now using the correlation dynamic shear modulus (G_a) is obtained. For saturated sandy soil specimen sheared under undrained loading condition, the Poisson ratio (ν) was assumed to be 0.5 as per recommendation in the literature.

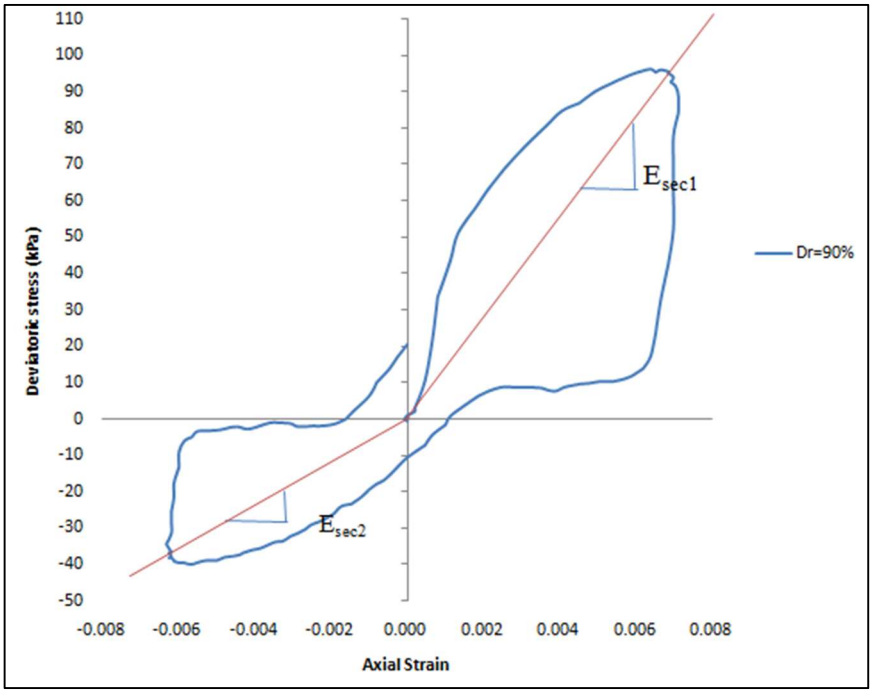

Fig.69: Plot of deviatoric stress Vs axial strain for Dr=90%, γ= 1.0% and f =1 Hz

- $E_{sec1}= \frac{56-0}{0.004-0}$= 14 GPa
- $E_{sec2}= \frac{24-0}{0.004-0}$= 6 GPa
- $E_{sec,a}= \frac{Esec1+Esec}{2} = \frac{14+6}{2}$= 10 GPa
- $G_{sec} = \frac{Esec}{2(1+\nu)} = \frac{10}{2(1+0.5)}$ = 3.33 GPa

4.2.4 Effect of shear strain on dynamic shear modulus

From the experimental data obtained, G from conventional method and G_a from modified method were evaluated based on the procedure described in the previous section. Figure 70 depicts the variation of shear modulus (G) with shear strain (γ) for soil specimen prepared at 60% relative density and sheared at a constant effective confining pressure of 100 kPa. It was observed that as the shear strain increases the shear modulus decreases. It means the at high shear strain the shear strength of the soil decreases. Subsequently, the potential for liquefaction of the soil increases.

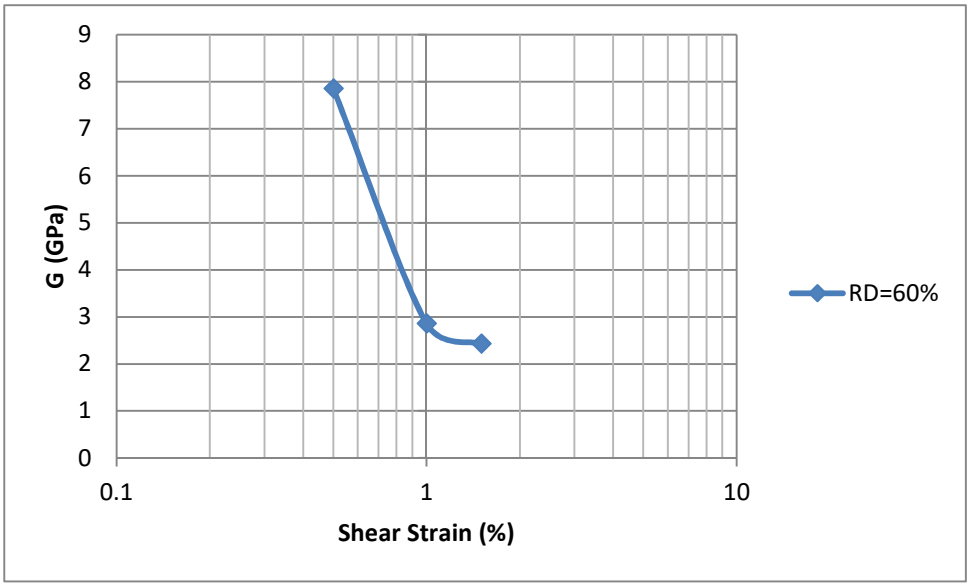

Fig.70: Variation of shear modulus (G) with shear strain (ϒ) for D_r = 60% and f= 1 Hz

Modulus degradation curve generally represent the degradation of shear modulus with shear strain. It is actually the variation of reduction in modulus ratio with increase in shear strain. G_{max} is the maximum shear modulus of the soil that is generally defined at a very low shear strain ($\Upsilon \leq 5 \times 10^{-6}$). For the present study, the shear strain used for the investigation was very high (0.5-1.5%). At this high value of shear strain, value of shear modulus was very low. So, to obtain the maximum shear modulus (G_{max}), the empirical co-relation given by the Hardin and Drnevich 1972 was used, which is expressed as

$$G_{max} = 102132.648 * \frac{(2.973-e)^2}{(1+e)} * (OCR)^K * (\sigma c')^{0.5}$$

Where, e is the void ratio, OCR is the overconsolidation ratio (for present study, OCR=1), σ_c' is the effective confining pressure, where σ_c' and G_{max} are in N/m^2.

Figure 71 represent the modulus degradation curve for the soil used in this study. The trend of modulus degradation curve obtained from the investigation was very much similar with the past research on the dynamic soil properties of Indian soil. G_{max} calculated for different relative density using the co-relation given by Hardin and Drnevich 1972 is shown in the table 3.

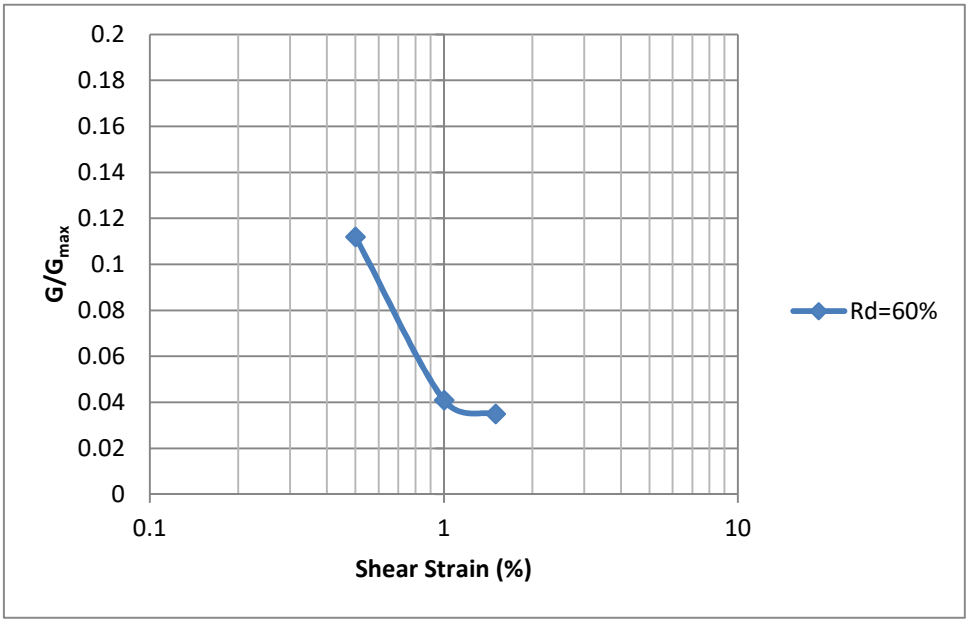

Fig.71: Modulus Degradation Curve for D_r = 60% and f= 1 Hz

Table 3: Value of maximum shear modulus for different relative density

Relative Density (D_r)	G_{max} (GPa)
35	55.39
60	70.06
75	80.45
90	92.28

4.2.5 Effect of relative density (D_r) on dynamic shear modulus (G)

Figure 72 presents the variation shear modulus (G) with different relative density i.e. 35%, 60%, 75% and 90%. As indicated in figure 72, increase in relative density increases the dynamic shear modulus. A trend line has been shown in the figure to show how shear modulus increases with relative density.

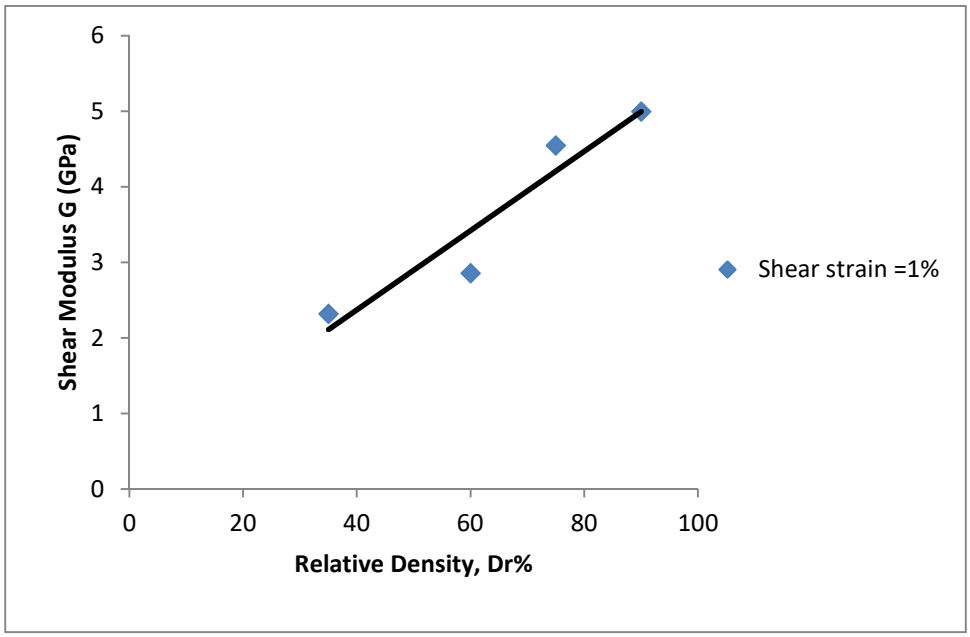

Fig.72: Plot of Shear modulus (G) Vs Relative Density (D_r) for γ= 1% and f= 1 Hz

4.2.6 Variation of Shear Modulus (G) with number of cycle (N)

Figure 73 depicts the variation of shear modulus with Number of cycle (N) for soil specimen prepared at 90% relative density and sheared at peak shear strain of 1%. The shear modulus for each hysteresis loop up to 25th cycle was determined using conventional method as discussed in the section 5.1. It was observed that as the number of cycle (N) increases, the dynamic shear modulus first decreases at very fast rate, the rate of decrease becomes very low. Hence the graph becomes flattered at high number of cycle.

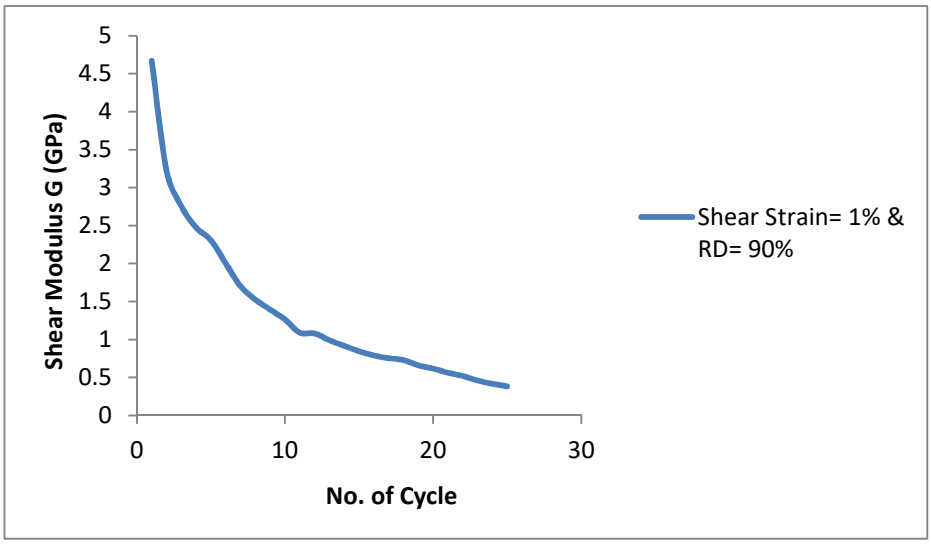

Fig.73:Variation of Shear Modulus (G) with number of cycle (N) at Dr=90% , ϒ= 1% and f= 1 Hz

4.2.7 Evaluation of damping ratio (D*) by modified method

To estimate the damping ratio (D*), the modified method for asymmetric hysteresis loop was used as indicated in Kumar et al 2017. In this method, the stored strain energy in one complete loop has been considered (represented by hatched polygon in the figure 66), which consist of two triangle and a rectangle having area $A_{\Delta 1}$, $A_{\Delta 2}$ and $A_{\square}$ respectively. Area enclosed by the hysteresis loop (A_L) is determined using the software called 'Hysteresis Loop Analysis' by Cui and Shen. Then using formulae given in the figure 66, the actual damping ratio was determined.

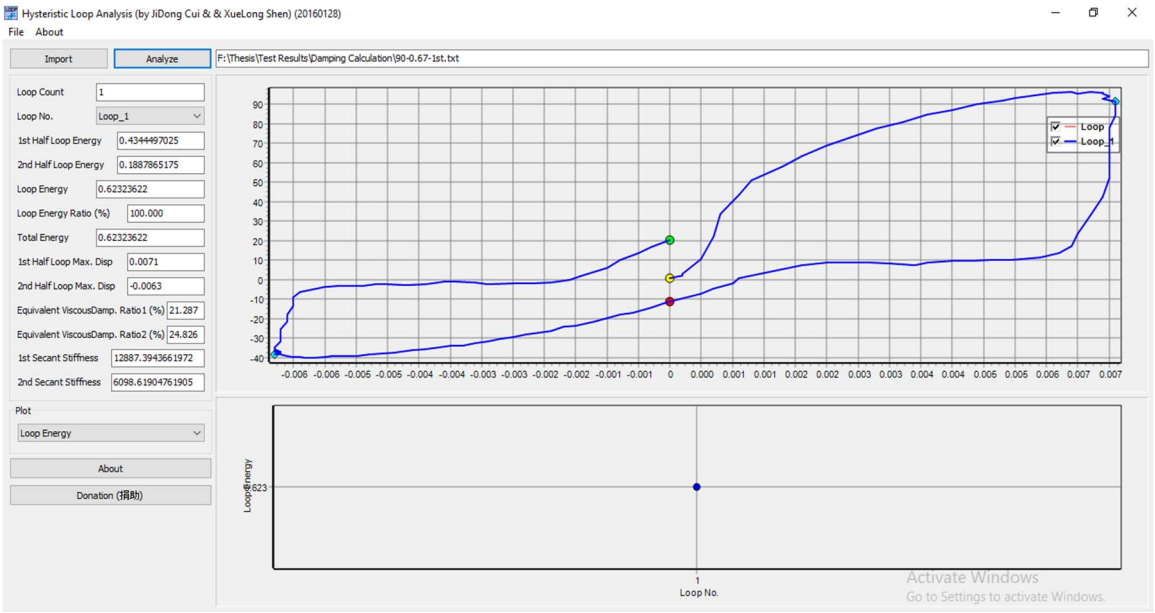

Fig.74: Determination of area enclosed by hysteresis loop by Hysteresis Loop Analysis software developed by Cui and Shen.

From figure 74 and 75:

- Area enclosed by the Hysteresis loop from the Hysteresis Loop Analysis Software, A_L = 0.62 kPa
- Area of Triangle, $A_{\Delta 1}$= 0.321 kPa
- Area of Triangle, $A_{\Delta 2}$= 0.116 kPa
- Area of the rectangle, $A_{\square}$= 0.257 kPa
- Total area $A_{\Delta 1}+ A_{\Delta 2}+ A_{\square}$=0.321+0.116+0.257=0.694 kPa
- So, damping ratio (D*) = $\frac{1}{\Pi} * \frac{AL}{A\Delta 1+A\Delta 1+ \square} = \frac{1}{\Pi} * \frac{0.62}{0.321+0.116+0.257}$=0.284=28.4%

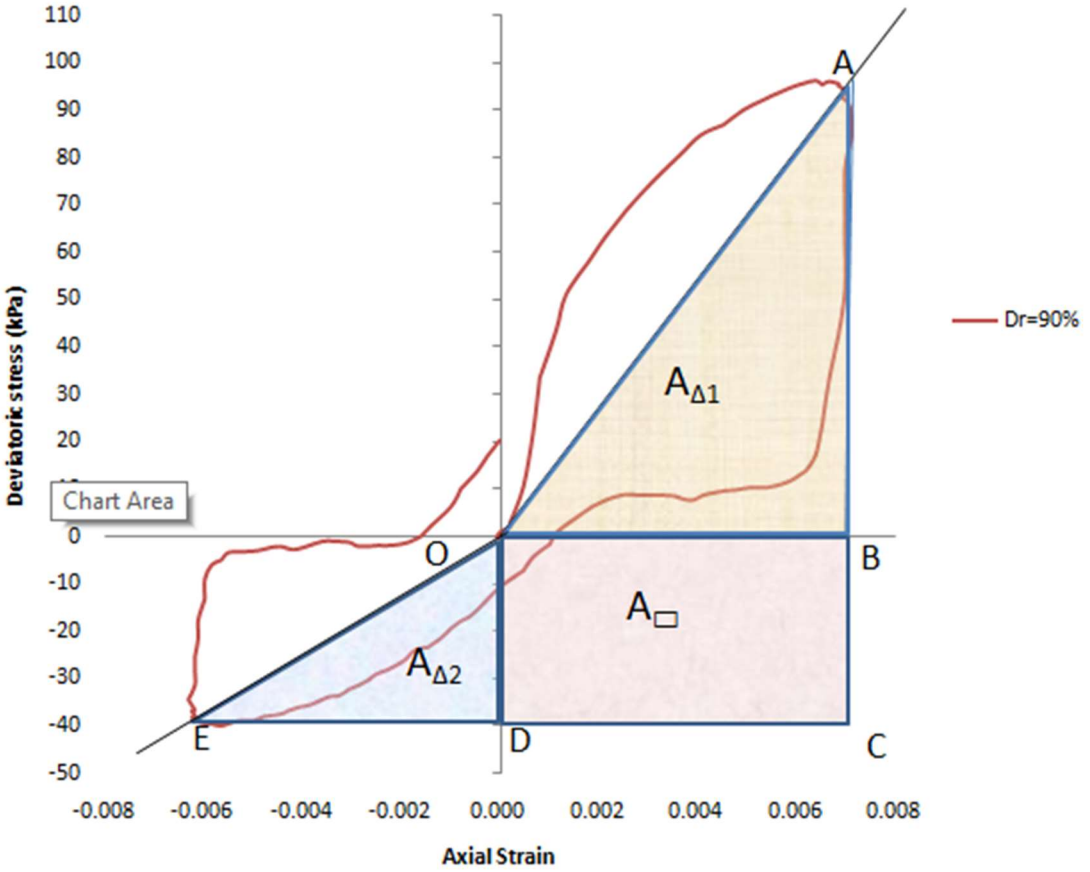

Fig.75: Determination of damping ratio (D*) by modified method for Dr = 90%, ϒ= 1% and f= 1 Hz

4.2.8 Effect of Shear strain (γ) on damping ratio (D)

Figure 76 present the variation of Damping ratio (D*) obtained by using modified as discussed in the previous section with the shear strain (γ) ranges from 0.5-1.5%. At this range of high shear strain, the damping ration is observed to be increases linearly with increase in shear strain. Damping ratio is the ability of soil to dissipate energy during any dynamic loading. Hence, with increase in shear strain ability of soil to dissipate energy increases.

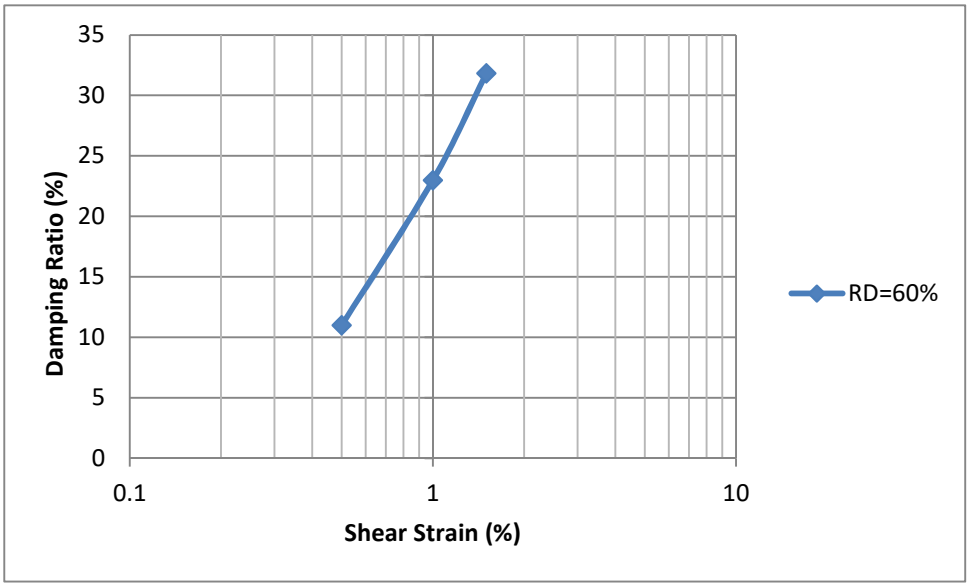

Fig.76: Plot of Damping ratio (D*) Vs Shear strain (γ) at Dr=60%, γ= 1% and f= 1 Hz

4.2.9 Variation of damping ratio (D*) with number of cycle (N)

Figure 77 depicts the variation of damping ratio (D*) with number of cycle (N) at relative density of 90% and peak shear strain of 1% up-to 10th cycle of loading it is observed that damping ratio decreases for first fast few cycle after that it decrease in the value of damping ratio becomes marginal.

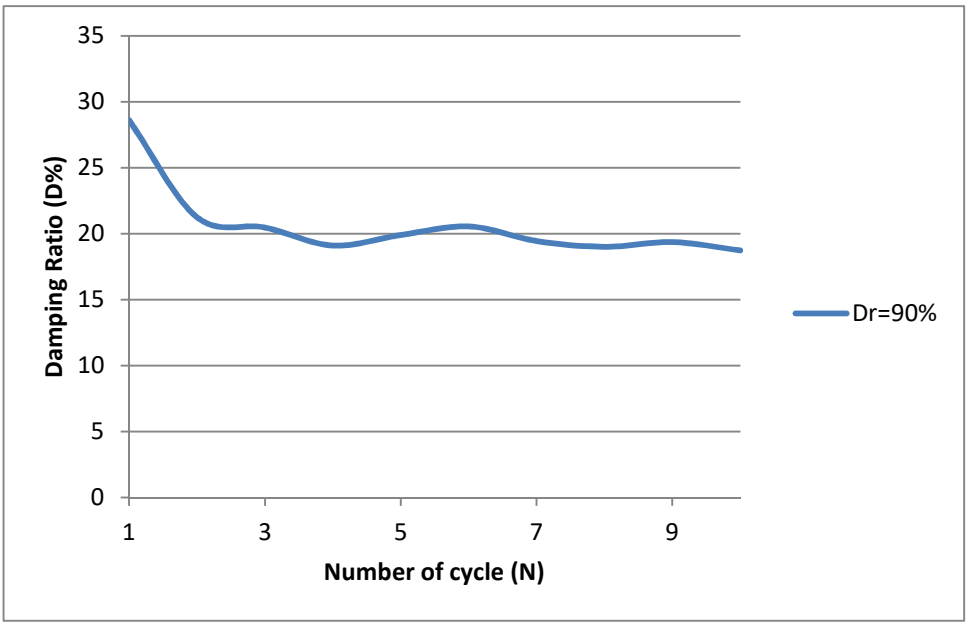

Fig.77: Variation of damping ratio with number of cycle (N) at Dr=90%,γ=1% and f=1Hz

5. Conclusions

The study presents the dynamic response of sandy soil of typical river channel deposit tested with different parametric variations using strain controlled cyclic triaxial test. The study considers the effect of relative density, shear strain amplitude and frequency of loading on liquefaction behaviour and dynamic soil properties of the soil. All the tests have been carried out at an effective confining pressure of 100 kPa. From the entire study, following conclusions are drawn:

(i) The study reveals that as the relative density increases, the liquefaction resistance of the sample also increases. This is quite intuitive, with higher relative density the soil moves into a denser packing increasing the liquefaction resistance of soil. The rate of generation of developed excess PWP is also observed to be quite lower for high relative density and it takes longer duration to reach liquefaction at same frequency and amplitude of loading. For example, at 1Hz loading frequency with 1% cyclic shear strain, the specimen with 90% RD reaches liquefaction at 50 cycles, whereas, for 35% RD, liquefaction is observed at 5 number of cycles.

(ii) The study exhibits a significant effect of peak cyclic shear strain on liquefaction resistance. As the peak shear strain increases, the number of cycle for liquefaction decreases. At 60% relative density with 0.5% shear strain, the number of cycles to reach liquefaction is found to be 100. On the other hand, at same relative density with 1.5% shear strain, liquefaction occurs only at 3 cycles. So, the impact of cyclic shear strain on liquefaction resistance of soil is substantial.

(iii) The tests have also been conducted to obtain the effect of frequency of loading. The results depict that as the loading frequency increases, the number of cycles to reach liquefaction also get increased at same shear strain amplitude. At loading frequencies of 0.1, 0.5 and 1 Hz, the failure cycles are observed to be 6, 12 and 20, respectively when the specimens are tested at 60% relative density with 1% shear strain. So, the study distinctly points out that the severity of loading increases at lower loading frequencies.

(iv) The study also determines the shear modulus and damping values of the soil at different parametric conditions. Shear modulus is observed to decrease quite rapidly with shear strain amplitude. The shear modulus exhibits a substantial reduction from 8 GPa to ~2.5GPa when the cyclic shear strain is increased from 0.5% to 1.5% at 60% relative density with 1Hz loading frequency. As it is already an established fact that with shear strain, soil losses its strength and the study also reveals the same. To represent the reduction in a popular non-dimensional form, plots have also been prepared between G/G_{max} and shear strain amplitude. The proposed modulus reduction curve can be used for any site specific analysis for the study region. Variation of shear modulus (G) of soil has also been presented with relative density and it shows that as the relative density increases, the shear modulus increases almost linearly. Further, it can be found that the shear modulus degrades with number of loading cycle.

(v) Damping ratio for the soil has been determined from the area of the hysteresis loop which is an indication of energy dissipation under the cyclic loading and represents the damping offered by the soil. For 60% relative density, it can be observed that the damping ratio increases almost linearly from 11% to ~32% when shear strain amplitude is increased from 0.5-1.5%. The curve represents the variation of damping ratio at high strain amplitude which is generally obtained from cyclic triaxial tests. The proposed curve can also be used for site specific dynamic response analysis in a combination with modulus reduction curve.

6. References

1. Ladd, R. S. (1978), "Preparing Test Specimens Using Undercompaction", Geotechnical Testing Journal, GTJODJ, 1(1): 16-23.
2. Kokusho T (1980), Cyclic triaxial test of dynamic soil properties for wide strain range. Soils and Foundation, 20 (2).
3. Seed HB, Wong RT, Idriss IM and Tokimatsu K (1986),"Moduli and damping factors for dynamic analysis of cohesionless soils", Journal of Geotechnical Engineering, 112(11): 1016–32.
4. Matasovic N and Vucetic M (1993), "Cyclic characterization of liquefiable sands", Journal of Geotechnical and Geoenvironmental Engineering,119:1805–22
5. Lade PV and Yamamuro JA (1997),"Effects of nonplastic fines on static liquefaction of sands", Canadian Geotechnival Journal, 34: 918–928
6. Lanzo G, Vucetic M and Doroudian M (1997)," Reduction of shear modulus at small strains in simple shear", Journal of Geotechnical and Geoenvironmental Engineering, 123:1035–42.
7. Vucetic M , Lanzo g and Doroudian M (1998), "Damping at small strain in cyclic simple shear test", Journal of Geotechnical and Geoenvironmental Engineering, 124:585–95.
8. Rollins KM, Evans MD, Diehl NB and Daily W D (1998), "Shear modulus and damping ratio for gravels", Journal of Geotechnical and Geoenvironmental Engineering, 124:396–405.
9. Polito CP and Martin JR II (2001), "Effects of no plastic fines on the Liquefaction resistance of sand", Journal of Geotechnical and Geoenvironmental Engineering, 127(5): 408-415
10. Xenaki VC and Athanasopoulos GA (2002), "Liquefaction resistance of sand–silt mixtures: an experimental investigation of the effect of fines", Soil Dynamics and Earthquake Engineering, 23:183–194
11. Naeini SA, Baziar MH (2004), " Effect of fines content on steady-state strength of mixed and layered samples of a sand", ELSEVIER , Soil Dynamics and Earthquake Engineering, 24 :181–187
12. Okur DV and Ansal A (2007) "Stiffness degradation of natural fine grained soils during cyclic loading", Soil Dynamics and Earthquake Engineering, 27:843–54.
13. Cubrinovski M and Rees S (2008), "Effects of Fines on Undrained Behaviour of Sands", Geotechnical Earthquake Engineering and Soil Dynamics IV Congress
14. Juneja A and Raghunandan ME (2010), "Effect of Sample Preparation on Strength of Sands", Indian Geotechnical Conference – 2010, GEOtrendz December 16–18, 2010 IGS Mumbai Chapter & IIT Bombay
15. Usmani A, Ramana GV and Sharma KG (2011), "Experimental Evaluation of Shear-Strength Behavior of Delhi Silt under Static Loading Conditions", Journal of Materials in Civil Engineering , 23(5): 533-541

16. Sachan A (2011), "Shear Testing Data of Soil: A function of Boundary Friction in Triaxial Setup", Indian Geotechnical Journal, 41(4), 168-176
17. Muley P, Maheshwari BK and Paul DK (2012), "Effect of Fines on Liquefaction Resistance of Solani Sand", 15th World Conference on Earthquake Engineering 2012
18. Roy N and Sahu RB (2012)," Site specific ground motion simulation and seismic response analysis for microzonation of Kolkata", Geomechanics and Engineering, 4 (1) 1-18
19. Salih AG and Kassim KA (2012), "Effective Shear Strength Parameters of Remoulded Residual Soil", EJGE,17, Bund. C
20. Mominul KM, Alam MJ, Ansary MA & Karim ME (2013), "Dynamic Properties and Liquefaction Potential of a Sandy Soil Containing Silt" ,18th International Conference on Soil Mechanics and Geotechnical Engineering, Paris 2013
21. Belkhatir M, Schanz T, Arab A (2013), "Effect of fines content and void ratio on the saturated hydraulic conductivity and undrained shear strength of sand–silt mixtures", Environmental Earth Science, 70:2469–2479 DOI 10.1007/s12665-013-2289-z
22. Kirar B and Maheshwari BK (2013), "Effect of Silt Content on Dynamics Properties of Solani Sand", Seventh International Conference on Case Histories in Geotechnical Engineering, Chicago
23. Hsiao DH and Phan VTA (2014),"Effects of silt contents on the static and dynamic properties of sand-silt mixtures" ,Geomechanics and Engineering, 7(3):297-316 ,DOI: http://dx.doi.org/10.12989/gae.2014.7.3.297
24. Karim ME and Alam MJ (2014),"Effect of non-plastic silt content on the liquefaction behaviour of sand–silt mixture", Soil Dynamics and Earthquake Engineering, 65:142–150
25. Kumar SS, Krishna AM, Dey A (2014), "Parameters Influencing Dynamic Soil Properties: A Review Treatise", International Journal of Innovative Research in Science, Engineering and Technology, 3 (4)
26. Kumar SS, Krishna AM, Dey A (2014), "Dynamic soil properties of Brahmaputra sand using Cyclic Triaxial tests", NES-Geocongress 2014
27. Kumar SS (2014), "Parameters influencing dynamic soil properties", IJIRSET ISSN (Online) : 2319 – 8753
28. Banupriya S, Soundarya M.K and Chakravarthy K (2015), "Stress-Strain and Strength Characteristics of Sand-Silt Mixtures", International Journal of Latest Trends in Engineering and Technology (IJLTET), 6 (1)
29. Kumar SS, Krishna AM and Dey A (2015),"Cyclic Response of sand using stress controlled cyclic triaxial test", 50th Indian Geotechnical Conference 2014
30. Vucetic M and Mortezaie A (2015), "Cyclic secant shear modulus versus pore water pressure in sands at small cyclic strains", Soil Dynamics and Earthquake Engineering , 70:60–72.

31. Dash HK and Sitharam TG (2016)," Effect of frequency of cyclic loading on liquefaction and dynamic properties of saturated sand", International Journal of Geotechnical Engineering, ISSN: 1938-6362

32. Kumar SS, Krishna AM and Dey A (2017), "Evaluation of dynamic properties of sandy soil at high cyclic strains", Soil Dynamics and Earthquake Engineering , 99 :157–167
33. Karim ME and Alam MJ (2017)," Efect of nonplastic silt content on undrained shear strength of sand–silt mixtures", International Journal of Geo-Engineering , 8:14
34. Varghese R, Amuthan MS, Boominathan A and Banerjee S (2019), "Cyclic and postcyclic behaviour of silts and silty sands from the Indo Gangetic Plain", Soil Dynamics and Earthquake Engineering, 125 :105750

35. Kumar SS, Krishna AM and Dey A (2020a), "Evaluation of monotonic and dynamic shear modulus of sand using on-sample transducers in cyclic triaxial apparatus", Acta Geotechnica, 16:221–236 https://doi.org/10.1007/s11440-020-01035-2
36. Kumar SS, Krishna AM and Dey A (2020b),"Monotonic and dynamic properties of riverbed sand and hill-slope soils of seismically active North-east India for ground engineering applications", International Journal of Geo-Engineering ,11:(9)
37. Chakrabortty P, Roshan AR and Das A (2020)," Evaluation of Dynamic Properties of Partially Saturated Sands Using Cyclic Triaxial Tests", Indian Geotech J, 50(6):948–962
38. Debnath R, Saha R, Halda S and Patra SK (2022)," Seismic site response analysis of Indo-Bangla railway site at Agartala incorporating site-specific dynamic soil properties", Bulletin of Engineering Geology and the Environment, 81:239, https://doi.org/10.1007/s10064-022-02717-9
39. Tafili M, Knittel L, Gauger V, Wichtmann T and Stutz HS (2023), "Experimental study on monotonic to high-cyclic behaviour of sand-silt Mixtures", Acta Geotechnica, https://doi.org/10.1007/s11440-023-02126-6
40. Sharika S and Anitha Kumari SD (2023)," An Experimental Study on Static and Cyclic Undrained Behaviour of Gangetic Sand", Indian Geotech J https://doi.org/10.1007/s40098-023-00727-2
41. Sarkar D, Goudarzy M and Wichtmann T (2023), "Applicability of the concept of equivalent intergranular void ratio to sand-plastic fines mixtures below threshold fines content", Marine Georesources & Geotechnology, DOI: 10.1080/1064119X.2023.2244938
42. Park SS, Lee DE and Tran DKL (2024)," Effects of loading frequency and specimen size on the liquefaction resistance of clean sand", Geomechanics and Engineering, 37 (2) :123-133 https://doi.org/10.12989/gae.2024.37.2.123